美国 NASA 冰桥(IceBridge)科学计划:进展与展望

冯准准[1],程晓[1],康婧[1],惠凤鸣[1],刘岩[1],程铖[2],
王芳[1],王显威[3],赵晨[1],赵硕[1],陈廷彪[1]

1. 遥感科学国家重点实验室 北京师范大学,北京 100875;
2. 北京建筑工程学院,北京 100044;
3. 遥感科学国家重点实验室 中国科学院遥感与数字地球研究所,北京 100101

摘 要:美国 NASA 于 2009 年启动的 IceBridge"冰桥"科学计划利用航空平台搭载的多源遥感传感器已在极区获取了连续的、高质量的观测资料。本文从多源航空遥感传感器及其采集数据的角度,对冰桥(IceBridge)科学计划做了详细介绍。其航空平台搭载的遥感传感器大致可以分为数字相机、激光雷达、雷达、重力以及辅助设备 5 类。本文又从冰雪 3 维立体制图、冰盖高程变化监测与物质平衡估算、海冰厚度与分布时空变化探测、卫星遥感校正与验证等 4 个方面对冰桥极地多源航空遥感数据的应用研究做了展望。冰桥科学计划将会大大促进人类对于气候变暖背景下两极所发生变化的理解。

关键词:IceBridge,激光雷达,重力仪,南极,北极,航空遥感,全球变化

中图分类号:TP237 **文献标志码**:A

引用格式:冯准准,程晓,康婧,惠凤鸣,刘岩,程铖,王芳,王显威,赵晨,赵硕,陈廷彪. 2013. 美国 NASA 冰桥(IceBridge)科学计划:进展与展望. 遥感学报,17(2):399-422

Feng Z Z, Cheng X, Kang J, Hui F M, Liu Y, Cheng C, Wang F, Wang X W, Zhao C, Zhao S and Chen T B. 2013. Review of the NASA IceBridge mission: Progress and prospects. Journal of Remote Sensing, 17(2): 399-422

1 引 言

全球变化的研究建立在完整对地观测技术基础上即没有完整的对地观测数据,就没有全球变化研究(徐冠华 等,2010)。南北两极是地球系统的重要组成部分。南北极作为地球的两大冷源,是全球气候变化的驱动器和放大器,极区的快速变化改变了地球的热平衡结构,全球气候引发的强烈反馈,成为影响全球气候变化的最重要的因素。然而极区观测数据的严重稀缺却制约了地球系统模式向更高的准确度发展。

遥感技术是获得极区观测数据最有效的手段之一,能够全天时、大范围、定量化、长期连续监测极区环境变化。至今,专门针对极区研究和监测的卫星主要有美国国家航空航天局 NASA(National Aeronautics and Space Administration)的 ICESat-1 和欧空局的 CryoSat-2。CryoSat-2 于 2010 年 4 月升空,目前数据已经正式发布。ICESat-1 是 NASA 于 2003 年 1 月发射成功的一颗科学实验卫星,所搭载的主要传感器是 GLAS(Geoscience Laser Altimeter System),目标是为了测量冰盖物质平衡、云和气溶胶高度以及陆地地形和植被特性。然而,由于激光传感器损耗的原因,ICEsat-1 于 2009 年停止获取数据。而 ICEsat-2 计划最早到 2015 年才能发射,为了保证极地快速变化时期观测数据的时间连续性,NASA 于 2009-10-15 开展了冰桥科学计划项目,该项目计划从 2009 年—2015 年连续 6 年利用多源航空遥感传感器(包括机载激光雷达)来获取南北极的对地观测数据,以此来揭示地球南北极变化与全球变化的相互作用机制。

2 冰桥计划介绍

冰桥计划是在地球两极所进行的最大航空遥

收稿日期:2011-11-24;修订日期:2012-06-09

基金项目:国家自然科学基金项目(编号:41176163);中央高校基本科研业务费专项资金资助;南北极环境综合考察专项(编号:JDZX20110010)

第一作者简介:冯准准(1983—),硕士研究生,研究方向为遥感与全球变化。E-mail: f_zhun.whu@163.com

通信作者简介:程晓(1976—),教授,主要从事极地遥感、环境遥感与气候变化研究。E-mail: xcheng@bnu.edu.cn

感科学观测工程,该计划观测区域包括: 格陵兰岛与南极洲海岸线、南极半岛、南极内陆、阿拉斯加东南部冰川以及南北极的海冰区域,将融合多源航空遥感数据对南北两极冰盖、冰架以及海冰等极地要素的结构进行探测,比如利用激光雷达获取冰面信息,利用测高和穿透雷达测量冰雪厚度以及冰下基岩地形,利用重力仪观测到冰下湖泊的分布与大小,利用每年重复一次的观测就可多方位高质量地监测极地要素的变化特征。冰桥计划将在以下两方面对冰冻圈科学作出贡献:

(1) 极区中剧烈变化区域对于海冰特定区域的特征化以及冰盖物质平衡过程模型的建立非常关键,然而这些变化不随时间呈线性关系变化,因此重复观测就显得尤为重要。冰桥计划代替 ICESat-1,不仅能继续提供表面高程变化信息,而且能更高分辨率更详尽地描述研究区域的多方位变化特征。

(2) 航空遥感将为冰川模型提供重要的补充观测数据比如冰下地形、接地线位置以及冰雪厚度等,而这些参数很难从卫星遥感中获得。另外,这些参数对于提高气候变化模式下冰川动力学模型以及海平面升降模型的预测精度起着非常重要的作用。

执行冰桥计划的航空平台主要有 P-3B、DC-8、UAF Otter、BT-67 和国王 B-200 小型飞机等,这些航空平台所搭载的遥感传感器大概可分为数字相机、激光雷达、雷达、重力仪以及辅助设备 5 大类,其主要代表型号见表 1 所列。

表 1 冰桥采用的主要航空遥感传感器

仪器名称	作用
数字测图系统相机 DMS (Digital Mapping System Camera)	地表成像
双机连续光学成像仪 CAMBOT (Continuous Airborne Mapping by Optical Translator)	地表成像
激光雷达 ATM (Airborne Topography Mapper)	地形测量
植被激光雷达 LVIS (Laser Vegetation Imaging Sensor)	地形测量
激光雷达 UAF Lidar (University of Alaska Fairbanks Glacier Lidar)	地形测量
光子计数成像激光雷达 Sigma-Space Lidar (Sigma Space Photon Counting Imaging Lidar)	地形测量
雷达高度计(Ku-band Radar Altimeter)	高程测量
雪深测量雷达(Snow Radar)	冰上雪深度测量
雪累积雷达(Accumulation Radar)	年雪层厚度测量
多通道相干雷达测深仪 MCoRDS (Multichannel Coherent Radar Depth Sounder)	冰厚测量
高级雷达测冰剖面仪 PARIS (Pathfinder Advanced Radar Ice Sounder)	冰剖面测量
航空重力仪 AIRGrav(Sander/LDEO Airborne Gravimeter)	重力异常测量
航空重力仪 BGM-3(Bell BGM-3 Gravimeter)	重力异常测量
定位定姿仪 POS/AV 510 (Position/Avionics)	飞机位置姿态测量
气象观测仪 AMET NSERC(Airborne Meteorological Instruments)	气象参数获取
UCAR/EOL 大气成分观测仪(UCAR/EOL Atmospheric Chemistry Instruments)	大气成分获取

冰桥计划已成功获取了 2009、2010、2011 年南北极的航空遥感数据,图 1 为 2009 年的航空数据采集路线图。这些数据分为 5 个级别,其中 Level0 为原始数据,经过地理定位、误差校正等处理后形成 Level1 级别,继而进行地理要素提取形成初步产品 Level2 级别的数据,目前 Level1 数据以及部分 Level2 数据由美国国家冰雪数据中心 NSIDC(National Snow and Ice Data Center) 实时发布([2012 - 06 - 29] http://nsidc.org/icebridge/portal/) 。其后的 Level3 级别数据为科学应用的产品制图数据, Level4 级别为模型输出与预测结果。Level1 数据采用 WGS84 椭球体下的极立体投影进行地理定位,其中北极标准纬线为北纬 70°,中央经线为西经 45°; 而南极标准纬线采用南纬 71°,中央经线为本初子午线。

3 搭载传感器及其数据产品介绍

3.1 光学传感器

光学遥感作为传统的遥感手段在极地地貌影像制图、地物分类、冰川运动速度提取、海岸线变化监测、海冰面积与分布等方面起着重要作用。参与冰桥计划的航空光学遥感系统主要有 DMS 和 CAMBOT,其中 DMS 数据的航向重叠率达到 80%,结合平台定位定姿数据,可以用于高精度的立体摄影测量。

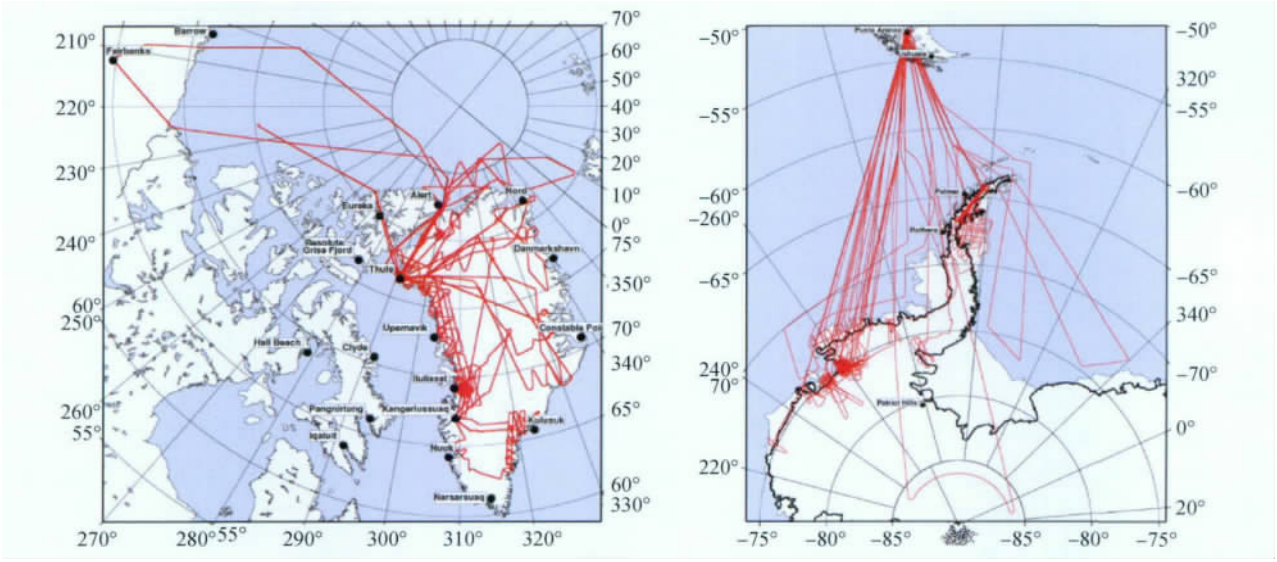

图 1 冰桥计划 2009 年南北极数据采集路线图(Koenig **等,** 2010)

3.1.1 DMS

DMS 是一套适用于中低空平台搭载的数字摄影测量系统,用于获取高分辨率的彩色和全色波段影像。该系统核心是一台佳能 EOS 5D Mark Ⅱ数码相机,相机配置佳能 F1.8 式 28 mm 的镜头,视场角为70°,并采用佳能自主研发生产的 36 mm × 24 mm CMOS 图像感应器,实现了约 2110 万有效像元的高影像质量和约 3.9 张/秒的高速连拍性能; 同时还配备了 9 个自动对焦点和 6 个辅助对焦点,能够在高速移动中捕捉目标; 其最终产生的影像大小为 5616 × 3744 个像元,具体摄影测量参数见表 2。

表 2 DMS 摄影测量参数表

高度/m	焦距/mm	旁向视场角/(°)	航向视场角/(°)	最低点影像分辨率/m	刈幅长度/m	刈幅宽度/m	面积/km^2
457.2	28	64.0	45.2	0.10	571	381	0.57
12192	28	64.0	45.2	2.71	15239	10160	400.81
12192	85	23.3	15.6	0.89	5020	3347	43.49

DMS 数据产品主要有两种,L0 级数据是 DMS 照相机直接获取的原始影像,未经处理,以 JPEG 格式存储; L1B 级数据(IODMS1B)是将原始数据经过几何定位和正射校正的影像。处理后的每景影像的摄影测量值都直接写入到图像文件中,包括坐标和投影信息、GPS 日期和时间、俯仰角、翻滚角、海拔高、快门速度和成像模式等,最后以 GEOTIFF 格式存储。以上两种产品自 2009 - 10 - 16 起已通过 FTP 向用户提供。

3.1.2 CAMBOT

CAMBOT 是由两台同步工作的柯达 DC4800 数码相机外加 GPS 和控制单元组成,其中柯达 DC4800 的镜头为 35 mm,曝光时间可达到 0.7 s,可产生大小为 2160 × 1440 共 330 万个像元的影像。CAMBOT 有两种工作模式: 连续拍摄和并行拍摄。连续拍摄模式下第 1 台相机以每 10 m 一景影像的速率拍出连续画面。当第 1 台相机的闪存卡满了之后,系统将切换到第 2 台照相机工作,同时第 1 台照相机将闪存卡中的影像传到计算机中。在并行模式下,这两款相机在光学转换器的控制下同时工作,每 5 m 交替各自拍摄一景影像。CAMBOT 系统每运行一次,就会记录 GPS 信息和影像信息,并分别存储在两个文件中,在后期处理时用时间信息把这两个文件关联起来,这就形成了经过地理定标的 Level 1B 级影像数据,与之关联的文本文件包含以下信息: 获取时间、中心经纬度、高程、相对航高、ATM 测距、俯仰角、翻滚角和偏航角。这些数据作为 NASA 冰桥实施项目的一部分被存储为 ASCII 文本文件(导航数据)、PNG 和 JPEG 格式(影像数据),从 2009 - 03 - 31 开始通过 FTP 进行发布。

3.2 激光雷达传感器

激光雷达传感器是冰桥计划数据采集的主力军,主要用于不断变化的南北极冰盖和冰川表面测

量,继而来监测冰盖等极地要素物质平衡的季节性和年际间变化、地表过程以及冰流之间净物质平衡的长期变化趋势,其他用途包括海冰高度测量,卫星激光雷达的校正,海面高度和海浪特征测量等。其中参与冰桥计划的 ATM 激光雷达由于其在冰川学上的应用近 20 年(Krabill 等,1995),成为建立长时间序列观测的关键;中高空搭载的 LVIS 激光雷达则在监测区域大面积扩展覆盖上起着决定性作用(Blair 等,2010);UAF Lidar 则主要用来监测 Alaska 地区的山地冰川。另外 ICECAP(Investigating the Cryospheric Evolution of the Central Antarctic Plate)计划所搭载的 Sigma Space 光子计数 3 维成像激光雷达,作为在冰冻圈领域应用新技术,已被用于 ICESAT-2的研发任务(Krainak 等,2010)。从表 3 可以看出,Sigma Space Lidar 的各项参数都十分领先,将会成为极地航空传感器系统的重要组成部分。

表 3 4 种激光雷达设备在冰桥计划中的性能参数表

性能	ATM	LVIS	UAF	Sigma-Space
采集频率/Hz	5000	500—5000	10000	20000
扫描角度/(°)	±15	±12	±30	±26
扫描频率/Hz	20	10	20	20
激光波段/nm	532	1064	905	532
脉冲宽度/ns	—	8	—	—
脚点大小/m	1	20	0.20	—
脚点间距	4—7 m	10—20 m	1 m	水平:15 cm 垂直:3 cm
刈幅	140—250 m	2 km	500—600 m	400 m

3.2.1 ATM

ATM 激光雷达是执行此次冰桥任务所搭载的主要遥感传感器之一。ATM 由美国 NASA 研制,自 1993 年起用于格陵兰岛的高程变化数据采集,经过改进,目前用于 IceBridge 计划的为其第 3 代产品,至今仍是用于冰川学测量的主要工具。飞行高度为 800—1400 m,结合全球定位系统(GPS)和惯性导航系统(INS),ATM 的测量精度可以达到 10 cm(Krabill 等,2002)。为了飞行轨迹精确地辅助 ATM 数据获取,NASA 还研制了相应的飞行管理系统,使 ATM 的测量精度进一步提高。ATM 的扫描方式比较特别,采用圆锥扫描,其激光脚点在地面形成一系列有一定重叠度的椭圆。原始激光斜距数据采集后,经过处理,形成大端法(高位字节排放在内存的低地址端,低位字节排放在内存的高地址端的数据存储方式)存储的 qi 二进制 Level1 文件,其内容包括:GPS 时间、经纬度坐标、高程、激光发射强度、回波强度、平台姿态角度、GPS 精度以及脉冲宽度;同时 NSIDC 也发布了 ATM 的 Level2 文本格式数据,其内容包括:时间、经纬度、高程、南北向坡度、西东向坡度、精度、窗口大小及位置、航线号。

3.2.2 LVIS

LVIS 是一种适用于中高空飞行搭载、且能生成中尺度光斑、全数字波形的机载激光雷达设备,由 NASA 戈达德空间飞行中心 GSFC(Goddard Space Flight Center)设计研发和应用,是美国 NASA 最先应用波形分析技术的代表。波形激光雷达通过数字化记录仪对整个回波进行采样,分别获取每个脉冲与地表相互作用后信号在时间轴上的振幅信息,形成较为完整的波形剖面。利用此技术采集得到的波形数据比使用离散回波获得的地物信息更丰富,特别是对于植被,可以获取更加详细的垂直方向信息。LVIS 激光雷达主要用于表面地形精确制图和测量多尺度的冰面垂直空间结构(Hofton 等,2010),如图 2 所示。其初步评估精度为 7 cm(Hofton 等,2009)。利用多时相相同地点的波形信息进行对比,就可获得该冰面的变化信息。冰桥计划发布的 LVIS 数据包括 Level 0 级原始数据、Level 1B 级波形数据和 Level 2 级点云产品数据,其中

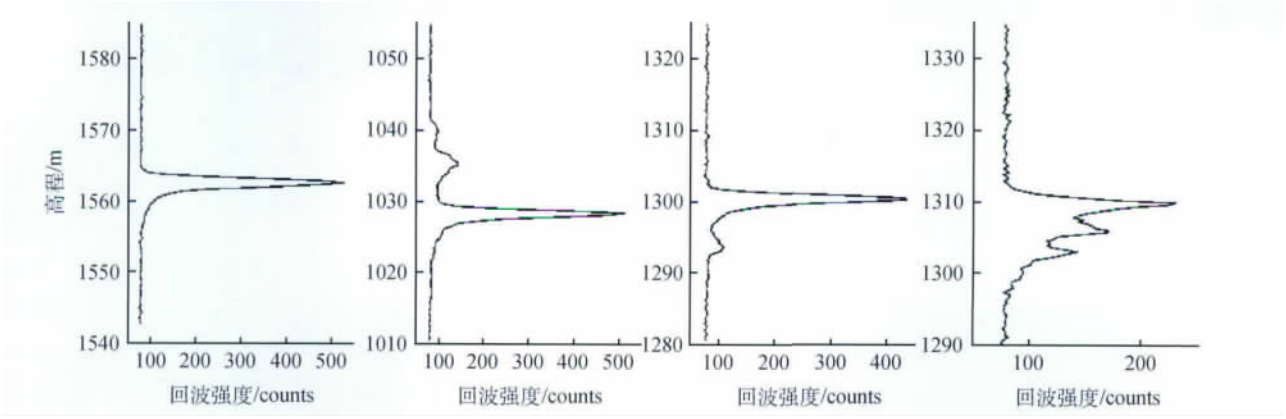

图 2 冰面的激光雷达回波特性示例(Blair 等,2010)

Level 2 级点云产品数据内容包括: 点 ID、GPS 时间、经纬度、高程、回波完全反射时的高度。

3.2.3 UAF Lidar

UAF (University of Alaska Fairbanks) 激光雷达系统是由 RIEGL LMS-Q240i 激光扫描仪、OxTS(Oxford Technical Solution) 惯导单元以及 Trimble GPS3 部分组成(UAF, 2006),其系统集成后冰川的高程测量精度可达到 10 cm(Larsen 等, 2009)。该雷达已被用于监测阿拉斯加附近的山地冰川近 20 年(Larsen 等, 2010),于 2009 年起加入冰桥计划,并在此前观测的基础上于每年的 5 月份以及 8 月份进行数据采集,目前已成功获取并发布了 2009 和 2010 年 UAF 激光雷达数据。RIEGL 激光扫描仪采用旋转多面体棱镜技术使其扫描脚点在地面上形成相互平行的扫描线,并将结果以二进制格式存储在 PC 机上。

在冰桥计划中采集的数据经过预处理后形成冰川剖面数据(共包含 25 条冰川) 以及扫描数据(共包含 29 条冰川),分别以 LAS 格式进行存储,且每个文件以指定冰川相应时间的数据进行创建,其内容包括: WGS84 坐标系下 UTM 投影的 X、Y、Z 坐标以及回波强度信息等。

3.2.4 Sigma-Space Lidar

Sigma-Space 光子计数 3 维成像激光雷达采用高重频、低脉冲能量的激光发射机和光电倍增式单光子探测器,把对目标的探测转换为对光子的计数,相比于波形探测更为选进,能充分利用激光回波脉冲中的光子能量,极大地提高了成像激光雷达的探测效率。Sigma-Space 光子计数 3 维成像激光雷达采用了被动式衍射光学元件,该光学元件以 80% 的效率把发射的激光脉冲分散为 10×10 阵列的 100 个细光束(所谓光子),这样每个光子包含超过 1 mW 的能量(~50 nJ @ 22 kHz)。这些细光束的回波被一个 10×10 阵列的光电倍增管阴极接收后,光电倍增管的阳极会把回波信号输送到精度为 2 ns 的多通道多节点的时间间隔测量系统去计时,而后利用发射信号与回波信号的时间差,就可求得测距,这样可一次得到 10×10 个激光脚点的 3 维场景。这些场景在数据采集过程中会被该激光雷达系统以每秒 220 万像元的速度不断地进行融合(Degnan等, 2007)。该系统初步估算的测距精度为 6 cm(Degnan, 2010)。另外值得注意的是,Sigma-Space 光子计数成像激光雷达把从发射到回波返回这段时间内所有光子,包括随机背景噪声(如太阳光子) 和信号都看作有效数据记录下来,因此 Sigma-Space 公司自行开发了一套滤波算法将有效测距数据从记录数据中提取出来(图 3)。

光子计数成像激光雷达不仅可以穿透树冠和大气雾霭,而且由于波长处于绿光波段还可以穿透一定厚度的水层,从而探测被水覆盖地表的地形特征,如图 3 所示,除得到融池的水表面信息外(绿点) 还能穿透水层得到融池底部信息(蓝点),可获得融池的 3 维立体图像。目前冰桥计划已经发布 2009 年的南极原始数据,2010 年数据正在处理中。

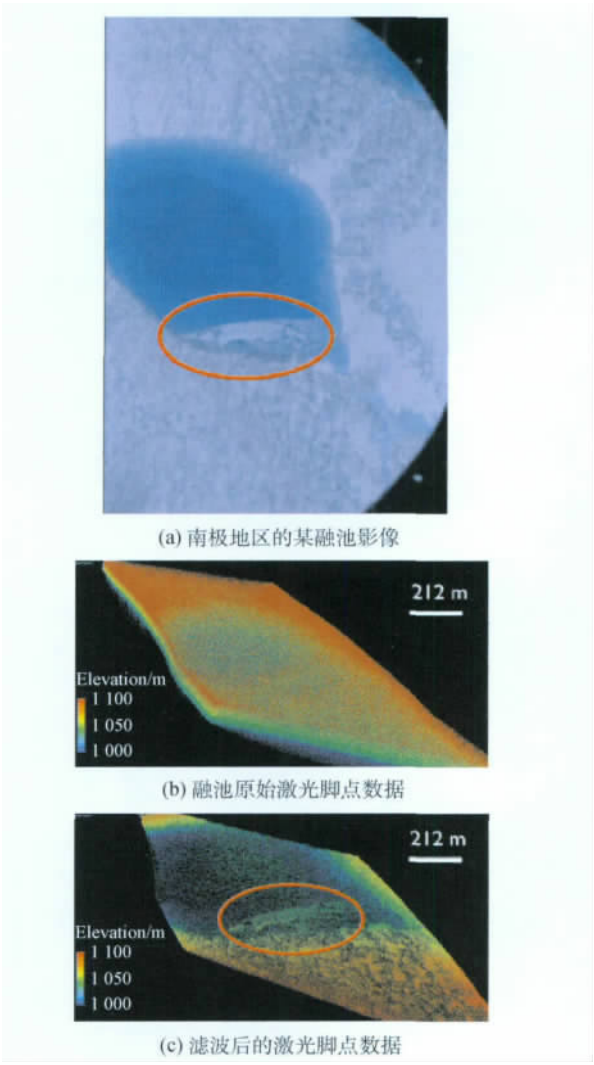

(a) 南极地区的某融池影像

(b) 融池原始激光脚点数据

(c) 滤波后的激光脚点数据

图 3 南极地区的某融池影像,该融池原始激光脚点数据,和滤波后的激光脚点数据(Degnan, 2010)

3.3 雷达传感器

众所周知,激光雷达只能获取冰层的表面信息,而为了更精确地获得冰盖总量的物质平衡以及解决冰川动力学的机理问题,就必须清楚地了解气-雪-冰-岩这几个关键要素的几何信息及 3 维分

布,比如雪累计量、海冰积雪厚度、冰盖厚度、基底地貌特征等参数,因此雷达探测在本计划中就显得至关重要。1993 年,美国堪萨斯大学研发了工作频段为 150 MHz 的回波雷达用来测量格陵兰岛冰盖的厚度(Leuschen 等, 2010) 。以堪萨斯大学为班底的冰盖遥感中心 CReSIS (The Center for Remote Sensing of Ice Sheets) 研发了一系列不同频段不同分辨率不同冰雪穿透能力的极地雷达仪器。冰桥计划采用的雷达仪器为 MCoRDS、Accumulation Radar、Snow Radar 和 Ku-band Radar。此外,约翰霍普金斯大学研发的 PARIS 仪器也在冰桥计划中得以应用,下面就这几款雷达设备做简要介绍(表 4) 。

表 4 冰桥计划中采用的几种雷达设备

设备名称	主要用途	频率(带宽)
MCoRDS	冰厚 冰下地形 冰层内部	195 MHz (30 MHz)
Accumulation radar	冰层近表面内部	750 MHz (300 MHz)
Snow radar	雪层冰层内部 冰面地形	4. 5 GHz (4 GHz)
Ku-Band radar altimeter	雪层冰面地形	14 GHz (4 GHz)
PARIS	冰层内部冰下地形	150 MHz(6 MHz)

3. 3. 1 Ku-band Radar Altimeter

Ku-band Radar Altimeter 是工作在 14 GHz 的宽波段雷达高度计,脉冲宽度在南极考察时为 170—240 μs,而在北极为 240 μs,脉冲重复频率为 3 KHz,发射功率为 20 dBm,采样频率为 62. 5 MHz。假定雪密度为 0. 5 g/cm^3,该雷达在格陵兰岛采集的数据距离分辨率可达 5. 3 cm,而在南极为 10. 6 cm。该雷达起初是为进行高精度冰盖表面高程测量而设计的,但最新研究(Willatt 等, 2011) 显示当积雪温度为 -4℃时,有 25% 的后向散射回波来自雪 - 冰交界面,而当积雪温度为 -8℃时,有 80% 的后向散射回波来自雪 - 冰界面,其余来自空气 - 雪界面,这表明随着温度的降低,Ku 波段雷达对积雪的穿透能力增强,因此在本次冰桥计划中该雷达除了进行表面高程测量外,还将与激光雷达数据一起使用来测算海冰上的积雪厚度。最新数据显示该雷达在冰盖近表层测量中可穿透 15 m 的粒雪层,而在海冰测量中可穿透约 0. 5 m 厚度的雪层(Patel 等, 2010) 。原始数据经过脉冲压缩、连冠整合、高通滤波、斑点去噪、高程修正等处理步骤后(Blake, 2010) ,存储为 bin 和 JPEG 格式,其中 bin 格式文件内容包括采集时间、经纬度、高程、冰表面回波时间、冰下回波时间、回波强度等,而 JPEG 格式文件为沿飞行路线的雷达冰雪数据剖面图。

3. 3. 2 Accumulation Radar

Accumulation Radar 是为量测雪累积量而设计的,其工作频段为 750 MHz,带宽 300 MHz,航空作业时的冰层内部分辨率为 28 cm,可以保证测量每年的雪累积厚度。另外,该雷达的扫描时程为 10 ms,发射功率 100 mW,采用蝶形阵列天线,采样频率 5 0 MHz,采用 12 位模/数转换器对信号进行处理。由 Accumulation Radar 获得的原始数据经过处理后存储为二进制格式文件并与 MATLAB 格式存储的 GPS 地理定位数据、Applanix 格式输出的航空平台定位定姿数据相关联。2010 年的北极地区数据已发布。

3. 3. 3 Snow Radar

Snow Radar 是由 CReSIS 研发的超宽频带雷达,其采用波频为 4. 5 GHz,脉冲宽度约为 250 μs,脉冲重复频率为 2 kHz,发射功率为 20 dBm,采样频率大概在 60 MHz 左右。假定雪密度为 0. 3 g/cm^3,该雷达在格陵兰岛采集的数据距离分辨率可达到 2. 5 cm,而在南极为 5. 25 cm(Panzer 等, 2010) 。该雷达主要应用于极地冰盖内层近表面粒雪层的高分辨率探测(图 4) 。此外由于雪厚度信息对于海冰物质平衡估算以及其表面能量交换有着重要影响,此雷达还被应用到南北极海冰积雪厚度及其时空分布的探测上(Kwok 等, 2010) 。本次冰桥计划收集的数据被存储为 bin 和 JPEG 格式,其中 bin 格式文件内容包括采集时间、经纬度、高程、冰表面回波时间、冰下回波时间、回波强度等,而 JPEG 格式文件内容为沿飞行路线的雷达冰雪数据剖面图。

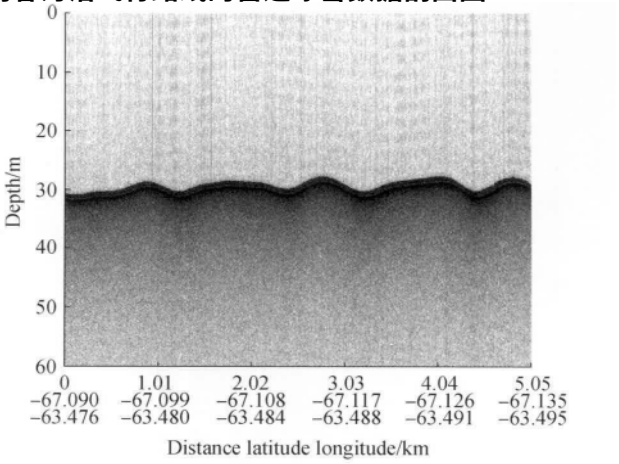

图 4 南极 Pine Island 岛地区的 snow radar 图 (Leuschen 和 Carl, 2011b)

3.3.4 MCoRDS

MCoRDS 是由 CReSIS 研发的多通道相干航空雷达,主要测量冰盖厚度和探测冰盖内层的雷达回波强度剖面信息,垂直空间分辨率为 4.2 m,其工作频段为 195 MHz,带宽为可调节式。此雷达配置多个接收通道可接收数字合成波束以提高杂波的识别能力,将削弱杂波对冰下岩层微弱回波信号以及冰下岩床条带状合成孔径雷达成像的影响(Lohoefener,2007)。另外,该雷达有 8 个通道,其中 5 个完全用来获取冰面与冰下岩石的回波信号,以测量冰厚;另外剩余的 3 个通道作为接收机与舱内天线相连接以测量电磁干扰信息,但是实验证明剩余的 3 个通道比上述 5 个通道能获取更多的冰表面回波信号,因此,通常情况下剩余的 3 个通道的数据用来估算冰厚,而冰厚的计算一般情况下是利用不同接收机中不同脉冲宽度的回波来分别测量冰表面与岩床传播时间之间的差异。

目前由 MCoRDS 获得的产品有 L1B 级的定位雷达回波强度剖面数据、L2 级的冰厚数据和 L3 级的冰厚、冰表面以及冰底部产品栅格数据。其中 L1B 级数据包括相对回波强度、时间、经纬度、高程、表面相对高度、飞机路线图以及雷达回波强度剖面图;这些数据存储在与 PNG、TIFF 和 pdf 格式文件相关的 mat 文件中(图 5)。而 L2 级冰厚度数据内容包括滤波处理后的经纬度、时间、表面高程、底部高程以及厚度信息。这些数据被存储在与 KML 文件相关联的 CSV 文本文件中。L3 数据产品则包括了飞行路线图、边界范围、格网值、预览图和交叉分析结果。这些数据被存储在 CSV 文本文件、PNG 文件、TIFF 文件、TFW 文件以及 ArcGIS 图层文件中。

3.3.5 PARIS

PARIS 雷达回波探测器是由约翰霍普金斯大学应用物理实验室研发的,首次实现了同类雷达的高空飞行测量(甚至适宜于星载探测),并且利用 150 MHz频段长波来对冰盖内部结构以及冰下地形进行探测(Raney 等,2008)。该雷达主要由高性能直接数字波频合成器、模拟/数字信号转换器以及可编码数据采集控制器 3 个部分组成,其中数字波频合成器负责脉冲的合成以及发射,模拟/数字信号转换器则接收来自天线的信号并进行转换,最后由数据采集控制器来完成对信号的处理与存储。

雷达接收到的信号不仅包括来自冰表面的主旁瓣反射信号和底部岩石的反射信号,还包括沿航线与垂直航线的杂波信号、冰层内部杂波信号以及

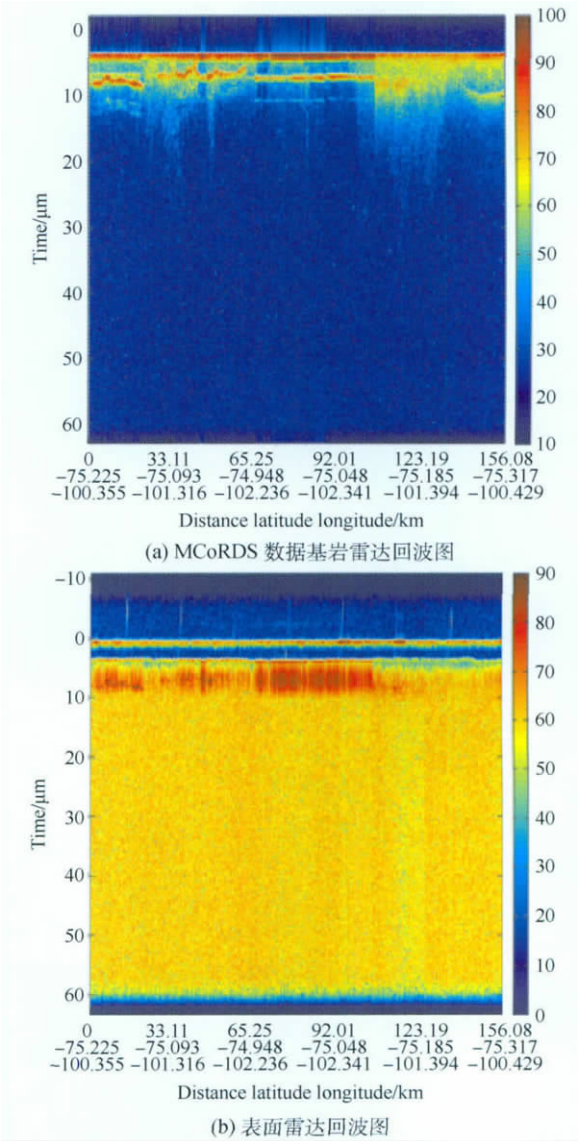

图 5 南极 Pine Island 地区的 MCoRDS 数据基岩雷达回波图与表面雷达回波图(NSIDC,2010a)

航空平台与表面的多次反射信号等噪声。约翰霍普金斯大学研究人员利用时延-部分相干多普勒频移滤波算法可有效地去除上述大部分噪声,如图 6 所示。处理后的雷达数据以文本格式存储为 L2 级冰厚度数据集进行发布,其内容包括经纬度、时间、冰厚、飞行高度以及数据可信度,其中数据可信度划分的 5 个等级由低到高分别描述数据质量。

3.4 航空重力仪

极地重力测量常用来进行冰下火山、断层以及地震等相关地质地貌特征的制图与解译。由于激光雷达只能测量冰的表面特征,且雷达虽然能穿透冰层测得冰间特征以及冰下地貌,但却无法测得冰

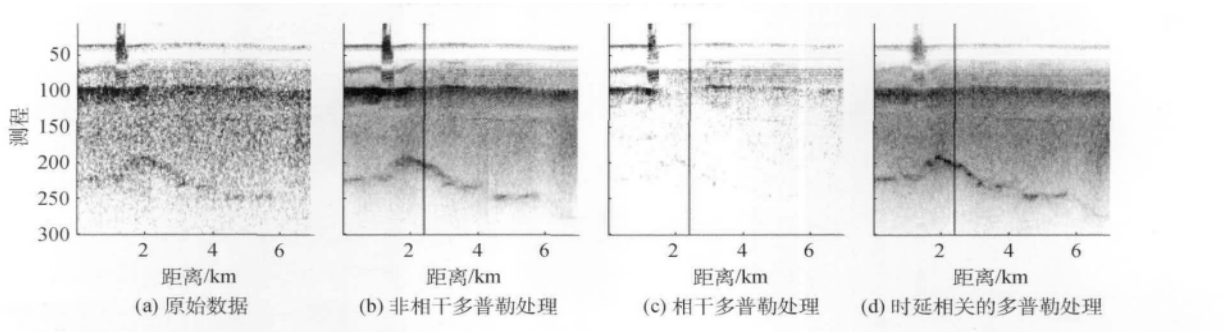

图 6 PARIS 雷达原始数据以及经过非相干多普勒处理、相干多普勒处理和时延 - 部分相关多普勒滤波算法处理后的效果对比图(Raney 等, 2008)

下水量,而这些冰下水体对整个冰层动态变化的作用不可忽视,因此极地重力测量也是评估冰下水影响机制的关键技术手段(Studinger 等, 2010) 。冰桥计划利用航空重力测量系统来评估冰舌下温暖海水对加速冰架底部消融的作用,同时重力测量也用来辅助雷达冰厚测量,冰下基底测绘以及海洋峡湾物探(Cochran 等, 2010) 。冰桥计划中重点监测区域包括格陵兰岛的 Petermann 冰川地区、Zachariae 冰川地区、Jakobshavn 冰川地区以及 Russell 冰川地区,还包括南极的 Abbot 冰架地区、Larson 冰架地区、南极半岛、Pine Island 冰川以及 Thwaites 冰川地区。

SGL 公司(Sander Geophysics Limited) 生产的 AIRGrav 航空重力系统是冰桥计划中的主要重力测量设备,是专门的航空重力仪,起初为石油勘探设计研发。该系统的核心是一个三轴陀螺仪稳定的惯性平台,装有 3 个互相垂直的精密加速度计作为重力传感器。惯性平台结合差分 GPS 来保证重力仪保持垂直,水平误差控制在 10 rad/s 之内,可以有效消除湍流、飞机抖动与起伏飞行带来的误差。采集到的原始重力数据经过解算、各种校正以及低通滤波后,精度可达到 0. 2 mGal,空间分辨率在 2. 2—4 km 之间(Sander 等, 2004) 。冰桥计划发布的重力测量数据包括区域重力数据以及每条航线的航空平台位置姿态数据,其中航空平台位置姿态数据以架次为单位进行文件划分发布,而区域重力数据则以上述重点监测地区为单位进行单独文件发布(其包含航线为作业线) ,其中还有一个文件专门存储冗余的航线数据,诸如飞机途经线、非作业区线、高度偏差过大线、飞行转弯线以及比对后遗弃线等,如图 7 所示。其重力数据包括: WGS84 坐标系下经纬度、日期、航线号、时间、极坐标投影 X、Y、椭球高、X、Y、Z 方向上加速度、布格校正、自由空气校正、航线间平差校正以及 70 s、100 s、140 s 低通滤波后的自由空间异常,还有航线间平差后的低通滤波自由空间异常。利用上述的各值就可以计算自由空间异常,用下式表示:

$$FAA = A_{\text{measured}} - A_{\text{aircraft}} + Eotvo + FAC - G_{\text{the}}$$

式中, FAA 为自由空间异常; A_{measured} 为实测重力; A_{aircraft} 为平台垂直加速度; $Eotvo$ 为布格校正; FAC 为自由空气校正; G_{the} 为正常重力值。

此外,Bell Aerospace 公司生产的 BGM-3 重力仪在 ICECAP 项目中被使用,这款重力仪起初为海洋重力测量设计研发,经过改进后应用到航空重力测量中。BGM-3 系统主要由强制反馈加速仪组成,其采样频率为 1 Hz,测程为 30 G。系统安置在陀螺稳定平台上,结合卫星导航,测量精度可达到 1 mGal (Richter 等, 2002) 。冰桥计划中,该系统贡献的是南极东南部地区的重力测量数据。自 2009 年起项目实时发布的数据包括以文本格式存储的 Level 0 级原始数据、L1B 级时间标记的加速度数据以及 L2 级地理定位的自由空气异常数据。

3. 5 辅助传感器

3. 5. 1 POS/AV 510 平台定位定姿传感器

搭载在航空平台上的许多仪器的测量结果都受平台姿态影响,于是提供高精度的平台定位定姿数据是整个项目测量的基础保障。冰桥计划采用加拿大的 POS/AV 510 系统来对航空平台进行轨迹校正,该系统是目前最先进的航空惯导系统,经过后期 GNSS 数据与 IMU(Inertial Measurement Unit) 数据融合处理后,其定位绝对精度可达到 5 cm,翻滚角与俯仰角的绝对精度可达到 0. 005°,而偏航角可达到 0. 008°(Mostafa 和 Hutton, 2002) 。在执行任务时,POS/AV 系统跟 DMS 耦合在一起进行操作,此种方式采集到的定位定姿数据可以应用到所有搭载仪器上去。发布的定位定姿数据是经过后期处理的

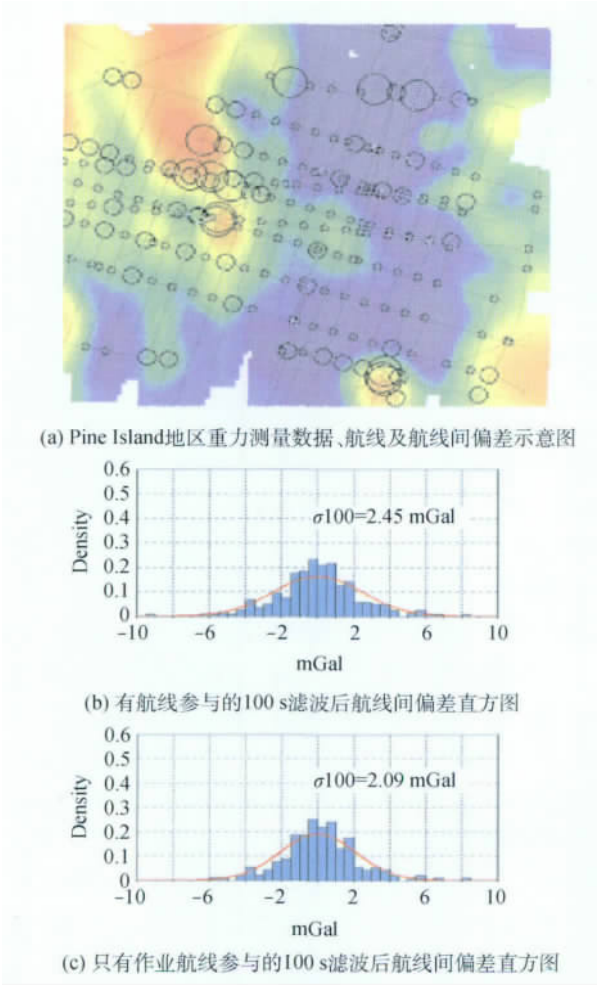

图7 Pine Island 地区重力测量数据、航线及航线间偏差示意图(圆大小表示)及航线间偏差直方图(Cochran 等,2011)

Level 1B 级数据,其包含的平台主要参数有:经纬度、高度、速度、翻滚角、俯仰角以及偏航角等。

3.5.2 NSERC 航空气象要素传感器

冰桥计划搭载了由 NSERC(National Suborbital Education & Research Center)提供的航空气象传感器系统,包括 MKS Baratron 220D 型压力传感器、Buck 湿度计系统、Edgetech137 型湿度计、Goodrich(Rosemount) 102 型总温测量仪以及 Heitronics 红外辐射高温计等用来测量大气、地表以及平台的气象要素高精度多源航空气象仪,且有太阳高度角、大气温度、大气压力、湿度、风、陆表温度、土壤温度、舱内压力以及仪表总温等在内的共 36 个参数测量。这些气象测量参数的数据采集频率超过 1 Hz,并用两个超大容量的 NASA 航空科学数据获取和传输飞行记录器进行记录。经过数据导出、格式转换以及质量控制等数据处理后,这些数据最终被存储为 ICARTT(Intercontinental Chemical Transport Experiment)格式文本文件,并于 2009 - 10 - 12 开始进行实时发布。

3.5.3 UCAR/EOL 大气成分测量传感器

除测量气象要素外,另一与气候变化密切相关的大气参数也被测量,即大气化学成分。该物理量主要是由 UCAR/EOL(National Center for Atmospheric Research /Earth Observing Laboratory)完成测量,其利用航空平台搭载 AVOCET 型非分散红外气体分析仪、机载差分吸收 CO 测量仪、二极管激光湿度计、机载空气样本采样器等仪器来测量南极上空大气中的 CO_2、CO、CH_4、N_2O、H_2O 以及其他气体成分的含量及分布(Yang 等,2010),产品以 ICARTT格式存储和发布。

4 冰桥观测数据应用

作为有史以来人类对地球两极最大的航空遥感观测科学工程,冰桥将结合 ICESat、Cryosat-2、ICESat-2建立大范围的长时间序列极区冰盖与海冰特征变化观测,并为南北两极快速变化区域提供重点监测,以此来帮助人类理解冰川运动过程,提高海平面上升模型的预测精度,下面从 4 个方面对冰桥计划数据的应用进行介绍。

4.1 冰雪 3 维立体制图

冰桥计划搭载的多源航空遥感传感器为全方位多角度探测极地地区物质组成及其分布提供了有利条件。利用激光雷达数据及光学影像可以获取表层地物覆盖及起伏信息。雷达数据则是探测冰层内部结构以及冰下地质地貌不可替代的遥感源,此外重力测量可以提供其他遥感手段探测不到的冰下溶洞、湖泊、水道等冰川特征的几何参数信息(Griggs 和 Bamber,2010; Hofton 等,2010; Richter 等,2002; Studinger 等,2010)。因此,融合多源航空遥感传感器数据将为极地科学研究提供无与伦比的基础支持。图 8 为利用 2009 年 IceBridge 项目采集的南极 Pine 岛冰川数据进行的 3 维立体制图,表层为 ATM 高程数据结合 Radarsat-1 SAR 影像形成的真实地表模型,底层为从 MCoRDS 雷达数据中反演的岩床地形模型,表面模型中的黄色箭头为从 Radarsat-1 数据中提取的冰流速,紫红色线条表示接地线,该图揭示了 Pine 岛冰川的厚度、支流分布以及冰川 - 海洋交互区域。另外,冰流速的走向和大小与冰下岩床的起伏相一致揭示

着冰流速随着冰厚的增加而改变很小。

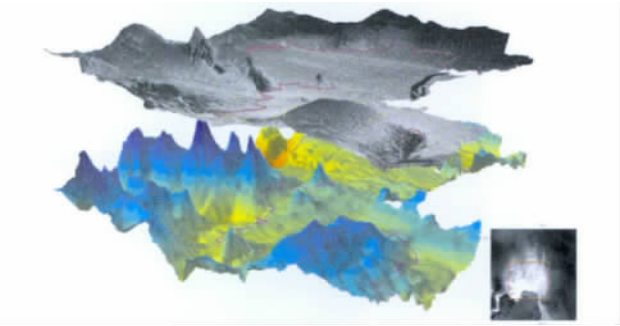

图 8 南极 Pine 岛冰川 3 维立体景观图(Blake 等, 2010)

利用高分辨率的 ATM 和 DMS 数据对西南极地区 Thwaites 冰架表面的冰裂隙进行了 3 维制图,如图 9 所示。

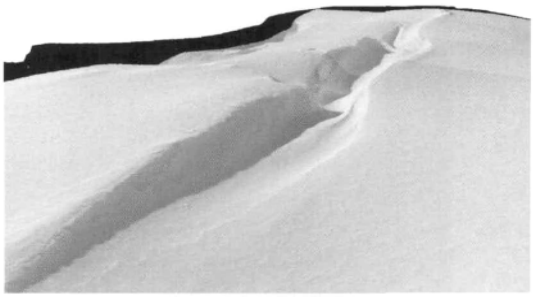

图 9 南极 Thwaits 冰架上某条冰裂隙的表面 3 维图

目前,科学家们非常关注利用重力异常数据对冰架底部地形的制图上,并已取得重大进展。Tinto 和 Bell (2011) 利用冰桥航空重力数据反演的 Thwaites 冰川地区水深模型发现了接地线前段 40 km处的两个基岩隆起峰,并指出它们控制了 Thwaites 冰川的进化过程。Cochran 和 Bell(2012) 反演了 Larsen 冰架下大陆架的地形走势,成功地显示了海水的入侵通道和聚集区。Schodlok 等人(2012) 进一步揭示了 Pine 岛冰川的消融速率跟通道外部的绕极深海暖流息息相关,并利用冰桥数据模拟得到该冰架的消融速率为 28 ma^{-1}, 此结果比其他模型估算的要高但却最接近于遥感估算的结果。

4.2 冰盖高程变化监测及物质平衡估算

南北两极冰盖高程的变化是研究全球变化最直观的因子,对其进行监测的主要原理是利用不同时间、相同地区的重复高程观测来求其差异,继而结合冰雪物质密度分布通过积分法来求该地区的冰雪物质平衡,于是冰桥计划中的测高传感器例如激光雷达、雷达高度计等发挥巨大作用(Sonntag 和 Krabill, 2009) 。自 1993 年至今,UAF Lidar 已对阿拉斯加地区超过 200 条冰川进行了时间间隔为 3—5 年的监测,2009 年冰桥计划又对其中超过 40 条的冰川进行了重复观测,监测显示绝大多数冰川的消融速率比 5—10 年前加快了 2 倍以上(Larsen 等, 2009) ,如图 10 所示。最新研究显示阿拉斯加地区冰川每年的负物质平衡为 41.9 ± 8.6 km^3,可导致海平面上升 0.12 ± 0.02 mm(Berthier 等, 2010) 。

同理,利用重力仪对同一地区进行重复观测求得重力异常差异后继而通过积分法也可以直接获得该地区的物质平衡。另外,多源航空遥感数据的采集使得通量法求得冰雪物质平衡成为可能,例如本次冰桥计划采集的雷达冰厚数据可以用来测量冰川物质通量,而通过重力数据反演的冰架下海洋水深以及冰溶洞分布信息可以用来估算冰架与海洋之间交互作用的水通量,雷达积雪厚度以及粒雪层分布数据可以用来估算雪累积量。但美中不足的是冰桥冰厚数据在格陵兰岛有些重要地区并没有覆盖,而在南极沿别林斯高晋海地区采集的冰厚数据属于首次采集且无法建立时间序列,因此采用通量法估算物质平衡还需要其他卫星遥感数据以及气候 - 海洋 - 冰盖模型的参与(Rignot 等, 2010) 。

4.3 海冰厚度与分布的时空变化监测

海冰是对气候变化最为敏感的因子,因此研究极区海冰的动态变化具有十分重要的意义。利用 DMS 等光学影像、雷达和激光回波数据获取的海冰范围和厚度动态变化信息不仅有助于理解海冰的形成过程和位置,还有助于分析其在目前气候模式下演化过程。提取海冰厚度的主要原理是先利用高程数据对海冰出水高度进行提取,利用冰在海水中浮力的分析计算得到海冰出水高度与海冰厚度的关系,于是海冰厚度可以通过间接的方式计算出来(Kurtz 等, 2008) 。

$$H_f = H_{si} - H_{ss} = h_s + f_b$$

$$h_i = \frac{\rho_s}{\rho_w - \rho_i} h_s + \frac{\rho_w}{\rho_w - \rho_i} f_b$$

式中,ρ_i、ρ_s 和 ρ_w 分别代表冰、积雪与海水的密度; h_i 为海冰厚度; H_{si} 为海冰表面高程,利用激光雷达测高 ATM 数据可获得; H_{ss} 为海水表面高程,利用重力数据可拟合得到; h_s 为海冰表面积雪厚度,利用 Ku-band 雷达和 Snow 雷达可获得; f_b 代表海冰浮出水面部分到冰雪分界面的高度。

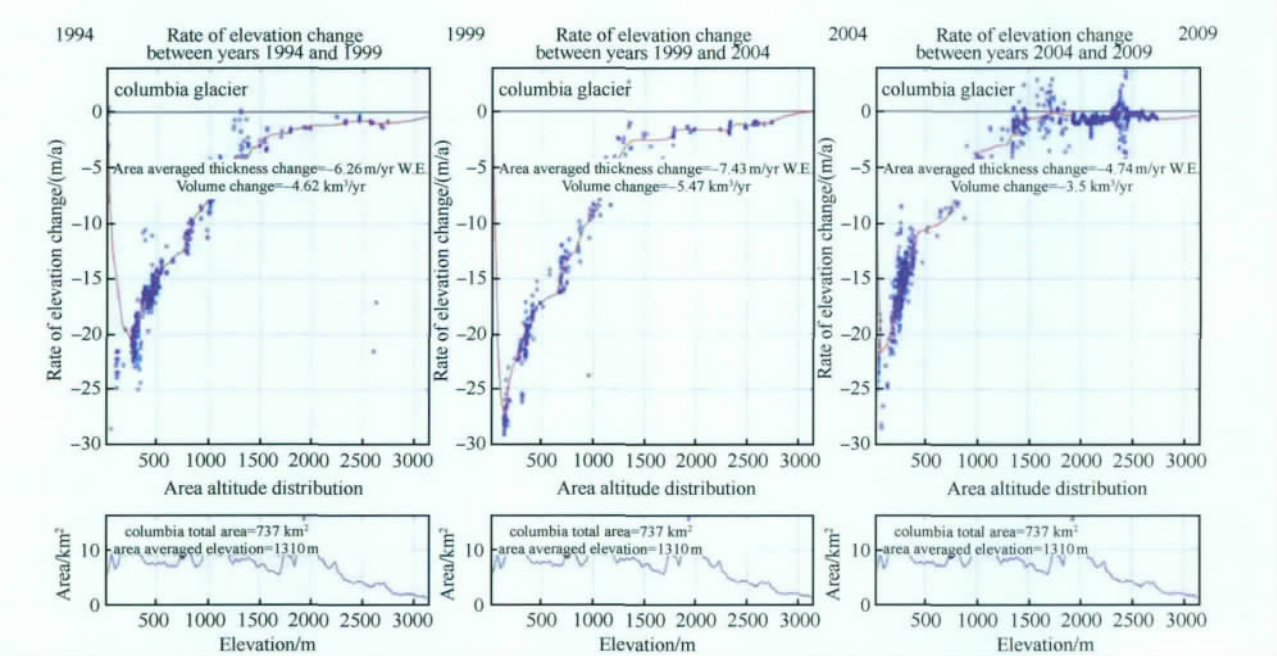

图 10 阿拉斯加地区哥伦比亚冰川 1994 年—2009 年高程变化以及高程 - 面积分布图(Larsen 等,2009)

4.4 卫星遥感观测校正与验证

冰桥计划每年将沿着 ICESat-1 卫星的运行轨迹进行 30 000 km 的海冰与冰盖数据采集,至少覆盖 5 00 km的 CryoSat-2 卫星轨迹。冰桥计划不仅会连接 ICESat-1 和 ICESat-2 卫星之间的冰盖高程数据以建立长时间序列的高程观测,而且将为激光雷达卫星(ICESat-1,CryoSat-2)和雷达卫星(CryoSat-2,Envisat)提供数据校正与验证,还会为未来发射的 ICESat-2 卫星和 DesDynI-Lidar 卫星进行仪器模拟实验与效果评估。在 2006 年进行的 Envisat/RA-2 雷达高度计验证任务中,NASA P-3 搭载的 ATM 与 RA-2 高度计测量的浮冰高度有着很高的一致相关性,平均差值 36 cm 被认为是来自浮冰上积雪厚度的影响,而在新冻结海冰上的差值为 1 cm(Connor 等,2009)。在 2010 年冰桥春季北极项目中,DC-8 搭载数字相机、激光雷达、雷达仪器沿 CryoSat-2 卫星轨道进行了验证活动(图 11),对 CryoSat-2 数据与冰桥数据进行了初步分析比较(Connor 等,2010)。

航空遥感数据有着精度高和分辨率高的特点,而卫星遥感数据则在大范围全局覆盖上有优势,空天遥感数据的交叉验证将会大大拓展冰桥数据的应用区域。当然,这些校正与验证也存在着由于地表类型、平台噪声以及覆盖范围不一致而引起的误差与不确定性(Connor 等,2009),另外航空遥感数据缺乏地面验证也是造成空天数据交叉验证

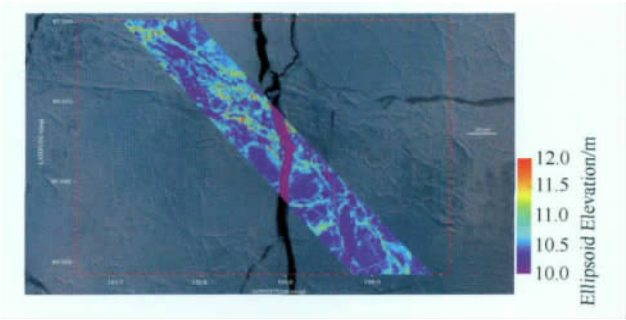

图 11 2010 年 4 月 20 日沿 CryoSat-2 轨道飞行的 ATM 以及 Cambot 海冰数据(Krabill,2011)

不确定性的因素之一。因此,利用冰桥数据建立空天遥感数据误差源、发展卫星校正与交叉验证的方法、改进相关算法将是未来研究的重点,也是空天遥感数据联合应用的前提与关键(Luthcke 等,2010)。

5 结 论

冰桥科学计划不仅会在时间上保证极地空天遥感数据的连续性,其搭载的多源航空遥感传感器也已经多角度、多方位地对极地要素进行了观测,这大大拓宽了人类对于极地要素变化机制理解的视野与思路。另外,从本文所述的 4 个应用方面可以看出,该科学计划的应用前景十分广阔。多源航空遥感数据的综合应用成为目前科学家们关心的问题,这不仅涉及不同尺度、不同传感器数据的融

合处理技术问题,其所呈现的极区应用整体实力也有待科学家们去评估与发掘。极地相关要素模型发展这一方面,诸如冰盖动力学模型、冰川动力学模型、海平面上升以及海冰覆盖模型的进一步发展都将需要从冰桥多源航空遥感数据提取的岩床地形、冰厚与冰结构、冰架或冰舌下水深、雪积累与结构、长时间序列南北两极快速变化等信息。

受航空后勤支持能力的限制,目前冰桥计划在南极的观测区域主要集中在西南极和南极半岛,在北极的观测区域主要集中在格陵兰岛的西部边缘地区。另外,受极区恶劣天气状况的影响,该项目航空遥感测量并没有达到传统意义上的工程测量要求,使获取的数据存在比例尺不一致的情况,从而增加了后期数据处理的难度。

自 1984 年以来,中国南极科学考察主要集中在南极半岛长城站附近和拉斯曼丘陵附近的埃默里冰架两个地区。同时,利用一船(雪龙船) 3 站(南极长城站、中山站、昆仑站) 所获得的极区数据相对较少,而中国的极区航空遥感能力正在建设中。由于冰桥计划生产的几乎所有产品都免费提供,少部分还可提供原始观测数据,因此,该项目不仅可以为中国科学家研究正在经历快速变化的西南极和北极地区提供海量的科学数据支撑,而且还可以为中国建设自主的航空遥感平台提供技术借鉴。

综上,利用冰桥计划连续时间序列的多源航空遥感数据,可以开展冰盖重要地区重要参数的动态监测,探测冰架与海冰变化机理,并为地球系统模式提供输入和验证数据。该科学计划不仅为开展多源航空遥感数据联合应用研究提供了宝贵资源,而且还对于了解全球变化的基本事实、探讨全球变化的客观规律有着重要意义。

志　谢　感谢美国 NASA 提供 IceBridge 观测数据。感谢 Texas A&M 大学的迟肇惠博士在 IceBridge数据下载方面提供的帮助。

参考文献(References)

Berthier E, Schiefer E, Clarke G K C, Menounos B and Rémy F. 2010. Contribution of Alaskan glaciers to sea-level rise derived from satellite imagery. Nature Geoscience, 3(2), 92 – 95

Blair J B, Hofton M A and Rabine D L. 2010. Large-area Ice Sheet and Sea Ice mapping from High-altitude Aircraft: Examples from the LVIS Sensor // American Geophysical Union, Fall Meeting 2010, abstract #C53A – 08, 08

Blake W A. 2010. Interferometric Synthetic Aperture Radar (InSAR) for Fine-Resolution Basal Ice sSheet Imaging. Lawrence: The University of Kansas

Blake W, Shi L, Meisel J, Allen C and Gogineni P. 2010. Airborne 3D basal DEM and ice thickness map of Pine Island Glacier. IEEE International Geoscience and Remote Sensing Symposium (IGARSS), 2010: 2503 – 2506 [DOI: 10.1109/IGARSS.2010.5653924]

Cochran J R, Bell R E, Frearson N and Elieff S. 2010. Inversion of IceBridge gravity data for continental shelf bathymetry beneath the Larsen ice shelf // American Geophysical Union, Fall Meeting 2010, abstract #C14A – 05, 05

Cochran J R and Bell R E. 2011. IceBridge Sander Air GRAV L1B Geolocated Free Air Gravity Anomalies. ed. IceBridge. Boulder, Colorado USA: National Snow and Ice Data Center (NSIDC)

Cochran J R and Bell R E. 2012. Inversion of IceBridge gravity data for continental shelf bathymetry beneath the Larsen ice shelf, Antarctica. Journal of Geodynamics, 58(209): 540 – 552 [DOI: 10.3189/2012JoG11J033]

Connor L N, Laxon S W, Ridout A L, Krabill W B and McAdoo D C. 2009. Comparison of Envisat radar and airborne laser altimeter measurements over Arctic sea ice. Remote Sensing of Environment, 113(3), 563 – 570 [DOI: 10.1016/j.rse.2008.10.015]

Connor L N, Laxon S, McAdoo D C, Farrell S L, Ridout A, Cullen R, Francis R, Studinger M, Krabill W B and Sonntag J G. 2010. A first comparison of CryoSat-2 and ICEBridge altimetry from April 20, 2010 over Arctic Sea Ice // American Geophysical Union, Fall Meeting 2010, abstract #C41A – 0506, 0506

Degnan J J, Wells D, Machan R and Leventhal E. 2007. Second generation airborne 3D imaging lidars based on photon counting // Advanced Photon Counting Techniques II, 67710N. Boston, MA, USA

Degnan J J. 2010. Photon Counting Lidars for Airborne and Spaceborne Topographic Mapping // Applications of Lasers for Sensing and Free Space Communications (LSC). San Diego, California: Optical Society of America

Griggs J and Bamber J. 2010. A new, multi-resolution bedrock elevation map of the Greenland ice sheet // American Geophysical Union, Fall Meeting 2010, abstract #C22B – 07, 07

Hofton M A, Luthcke S B, Blair J B, Rabine D and McIntosh C. 2009. Precise and Accurate High-Altitude Waveform Lidar Mapping of Greenland Land and Arctic Sea Ice in Support of Operation IceBridge // American Geophysical Union, Fall Meeting 2009, abstract #C51B – 0488, 0488

Hofton M A, Blair B, Luthcke S, Rabine D, McIntosh C and Beckley M. 2010. Characterizing Ice Sheet Surface Topography and Structure Using High-Altitude Waveform Airborne Laser Altimetry // American Geophysical Union, Fall Meeting 2010, abstract #C11A – 0523, 0523

Koenig L, Martin S, Studinger M and Sonntag J. 2010. Polar airborne observations fill gap in satellite data. Eos Transactions American Gerophysical Union, 91(38): 333 – 334 [DOI: 10.1029/2010EO380002]

Krabill W B, Thomas R H, Martin C F, Swift R N and Frederick E B.

1995. Accuracy of airborne laser altimetry over the Greenland ice sheet. International Journal of Remote Sensing, 16(7): 1211 – 1222 [DOI: 10.1080/01431169508954472]

Krabill W B, Abdalati W, Frederick E B, Manizade S S, Martin C F, Sonntag J G, Swift R N, Thomas R H and Yungel J G. 2002. Aircraft laser altimetry measurement of elevation changes of the Greenland ice sheet: Technique and accuracy assessment. Journal of Geodynamics, 34(3 – 4), 357 – 376 [DOI: 10.1016/S0264 – 3707(02)00040 – 6]

Krabill W B. 2011. IceBridge ATM L1B Qfit Elevation and Return Strength. IceBridge. Boulder, Colorado USA: National Snow and Ice Data Center (NSIDC)

Krainak M A, Yu A W, Yang G M, Li S X and Sun X L. 2010. Photon-counting detectors for space-based laser receivers // Razeghi M, Sudharsanan R and Brown G J. Proceedings of the SPIE 7608, 760827. San Francisco, California, USA

Kurtz N T, Markus T, Cavalieri D J, Krabill W, Sonntag J G and Miller J. 2008. Comparison of ICESat data with airborne laser altimeter measurements over Arctic sea ice. IEEE Transactions on Geoscience and Remote Sensing, 46(7): 1913 – 1924 [DOI: 10.1109/TGRS.2008.916639]

Kwok R, Leuschen C, Panzer B, Patel A, Kurtz N T, Markus T, Holt B and Gogineni P S. 2010. Radar surveys of snow depth over Arctic sea ice during Operation IceBridge // American Geophysical Union, Fall Meeting 2010, abstract #C21D – 02, 02

Larsen C, Hock R, Arendt A and Zirnheld S. 2009. Airborne Laser Altimetry Measurements of Glacier Wastage in Alaska and NW Canada // American Geophysical Union, Fall Meeting 2009, abstract #C23C – 0508, 0508

Larsen C F, Johnson A, Zirnheld S L and Claus P. 2010. Operation IceBridge Alaska // American Geophysical Union, Fall Meeting 2010, abstract #C22B – 08, 08

Leuschen and Carl. 2011a. IceBridge Accumulation Radar L1B Geolocated Radar Echo Strength Profiles. Boulder, Colorado USA: National Snow and Ice Data Center

Leuschen and Carl. 2011b. IceBridge Snow Radar L1B Geolocated Radar Echo Strength Profiles. Boulder, Colorado USA: National Snow and Ice Data Center

Leuschen C, Gogineni P S, Allen C, Paden J D, Hale R, Rodriguez-Morales F, Harish A, Seguin S, Arnold E, Blake W, Byers K, Crowe R, Lewis C, Panzer B, Patel A and Shi L. 2010. The CReSIS Radar Suite for Measurements of the Ice Sheets and Sea Ice during Operation Ice Bridge // American Geophysical Union, Fall Meeting 2010, abstract #C44A – 02, 02

Lohoefener A. 2007. Design and Development of a Multi-Channel Radar Depth Sounder. Lawrence: The University of Kansas

Luthcke S B, Rowlands D D, McCarthy J, Sabaka T J, Arendt A A, Loomis B and Boy J. 2010. Changes in Land Ice from GRACE: Signal, Errors and Relation to Other Missions // American Geophysical Union, Fall Meeting 2010, abstract #C43F – 08, 08

Mostafa M M R and Hutton J. 2002. Direct positioning and orientation systems: How do they work? What is the attainable accuracy. International Archives of Photogrammetry and Remote Sensing, 33

Panzer B, Leuschen C, Blake W, Crowe R, Patel A, Gogineni P S and Markus T. 2010. Wideband radar for airborne measurements of snow thickness on sea ice // American Geophysical Union, Fall Meeting 2010, abstract #C21D – 01, 01

Patel A, Gogineni P, Leuschen C, Rodriguez-Morales F and Panzer B. 2010. An Ultra Wide-Band Radar Altimeter for Ice Sheet Surface Elevation and Snow Cover Over Sea Ice Measurement // American Geophysical Union, Fall Meeting 2010, abstract # C41A – 0518, 0518

Raney R K, Leuschen C and Jose M. 2008. Pathfinder Advanced Radar Ice Sounder: PARIS // Geoscience and Remote Sensing Symposium, III-346-III-349. Boston, MA: IEEE

Richter T G, Kempf S D, Holt J W, Morse D L, Blankenship D D and Peters M E. 2002. Airborne gravimetry and laser altimetry over Lake Vostok, East Antarctica // American Geophysical Union, Spring Meeting 2002, abstract #B22A – 04, 04

Rignot E J, Schodlok M, Menemenlis D, Studinger M, Cochran J R and Bell R E. 2010. Improvements in the determination of ice sheet mass fluxes and freshwater fluxes using Icebridge data // American Geophysical Union, Fall Meeting 2010, abstract #C22B – 01, 01

Sander S, Argyle M, Elieff S, Ferguson S, Lavoie V and Sander L. 2004. The AIRGrav airborne gravity system // The ASEG-PESA airborne gravity 2004 workshop: Geoscience Australia Record, 49 – 54

Schodlok M P, Menemenlis D, Rignot E, Studinger M. 2012. Sensigivity of ice-shelf/ocean system to the sub-ice-shelf cavity shape measured by NASA IceBridge in Pine Island Glacier, West Antarcitca. Annals of Glaciology, 53(60): 156 – 162 [DOI: 10.3189/2012AoG60A073]

Sonntag J and Krabill W. 2009. Recent Changes in the Periphery of the Greenland Ice Sheet from NASA's Airborne Topographic Mapper // American Geophysical Union, Fall Meeting 2009, abstract #C43D – 05, 05

Studinger M, Allen C, Blake W, Shi L, Elieff S, Krabill W B, Sonntag J G, Martin S, Dutrieux P, Jenkins A and Bell R E. 2010. Mapping Pine Island Glacier's Sub-ice Cavity with Airborne Gravimetry // American Geophysical Union, Fall Meeting 2010, abstract #C11A – 0528, 0528

Tinto K J and Bell R E. 2011. Progressive unpinning of Thwaites Glacier from newly identified offshore ridge: Constraints from aerogravity. Geophysical Research Letters, 38: L20503 [DOI: 10.1029/2011GL049026]

Willatt R, Laxon S., Giles K, Cullen R, Haas C and Helm V. 2011. Ku-band radar penetration into snow cover on Arctic sea ice using airborne data. Annals of Glaciology, 52(57): 197 – 205

徐冠华, 宫鹏, 邵立勤, 林海, 戴永久, 王斌, 潘耀忠, 程晓. 2010. **我国全球变化研究急需加强的几个问题 //宫鹏 主编: 全球变化研究评论**, 1 – 11

Yang M M, Blake D R, Meinardi S, Vay S A, Choi Y, Rana M, Slate T, Sachse G W and Diskin G S. 2010. Chemical Composition of Tropospheric Air Mass Encountered During High Altitude Flight (> 11.5 km) over Antarctica at Latitude 86S During the 2009 Fall Operation Ice Bridge Field Campaign // American Geophysical Union, Fall Meeting 2010, abstract #A13B – 0194, 0194

Review of the NASA IceBridge mission: Progress and prospects

FENG Zhunzhun[1], CHENG Xiao[1], KANG Jing[1], HUI Fengming[1], LIU Yan[1], CHENG Cheng[2], WANG Fang[1], WANG Xianwei[3], ZHAO Chen[1], ZHAO Shuo[1], CHEN Tingbiao[1]

1. *College of Global Change and Earth System Science (GCESS), Beijing Normal University, Beijing* 100875, *China*;
2. *Beijing University of Civil Engineering and Architecture, Beijing* 100044, *China*;
3. *Institute of Remote Sensing and Digital Earth, Chinese Academy of Siences, Beijing* 100101, *China*

Abstract: This paper gives a detailed review of IceBridge mission, including the on-board multiple sensors employed, the collected data, and the different levels of products. The on-board multiple sensors can be divided into five types: digital camera, lidar altimeter, radar, gravimeter, and auxiliary equipment. Prospects of research based on IceBridge data are described in four aspects: three-dimensional mapping of snow or ice, changes in glacier elevation and estimates of mass balance, detection of changes in sea ice thickness and distribution, and calibration and validation of satellite remote sensing observations. IceBridge will undoubtedly enhance the understanding of polar changes under global warming.

Key words: IceBridge, Lidar, gravimeter, Antarctica, Arctic, airborne remote sensing, global change

CLC number: TP237 **Document code:** A

Citation format: **Feng Z Z, Cheng X, Kang J, Hui F M, Liu Y, Cheng C, Wang F, Wang X W, Zhao C, Zhao S and Chen T B. 2013. Review of the NASA IceBridge mission: Progress and prospects. Journal of Remote Sensing, 17(2): 399-422**

1 INTRODUCTION

Global change research is based on the full observation of the Earth. Thus, research without full Earth observation is not considered true global change research (Xu, et al., 2010).

Antarctica and the Arctic are significant components of the Earth system. As the two largest cold sources, they are the drivers and amplifiers of global climate change. Polar changes, which disrupt the Earth's heat balance structure and give strong feedback on the global climate, are the most important factors influencing global climate change. However, the severe scarcity of polar observations restricts further improvement of the Earth system model.

Remote sensing technology is one of the most efficient ways of monitoring polar regions because of its remarkable capability. Thus far, satellites specifically designed for polar observations include the ICESat-1, launched in January 2003 by NASA (National Aeronautics and Space Administration) of the USA, and CryoSat-2, launched in April 2010 by the European Space Agency. The main payload of ICESat-1 is its Geosciences Laser Altimeter System, which aims to measure the characteristics of ice mass balance, cloud and aerosol distribution, landforms, and forest height. CryoSat-2 data products have also been officially released.

With the gradual failure of three laser sensors, ICESat-1 stopped working in 2009. The new ICESat-2 satellite is scheduled to launch not earlier than 2015. To bridge the data gap in polar observations between ICESat-1 and ICESat-2, NASA initiated the IceBridge mission on October 15, 2009. This mission plans to use different types of airborne remote sensing instruments (including airborne lidar) to acquire annual polar observations from 2009 to 2015, helping scientists reveal the interaction mechanism between polar change and global change.

This paper gives a detailed review of this mission, including the multiple sensors employed, the collected data, and the different levels of data products, finally giving prospects of research based on IceBridge data.

2 ICEBRIDGE MISSION

IceBridge, a six-year NASA mission, is the largest airborne survey of Earth's polar ice ever flown. It uses airborne instruments to survey the Arctic and Antarctic regions once a year. Areas observed and measured by the IceBridge mission include coastal Greenland, coastal Antarctica, Antarctic Peninsula, interior Antarctica, the southeast Alaskan glaciers, and the Antarctic and Arctic sea ice. The NASA IceBridge mission combines multiple instruments to map ice surface topography, bedrock topography beneath the ice sheets, grounding line position, ice and snow thickness, and sea ice distribution and freeboard. Data from laser altimeters and radar sounders are paired with data from a gravimeter, magnetometer, mapping camera, and other data forms to provide dynamic, high-value, re-

Received: 2011-11-24; **Accepted:** 2012-06-09

Foundation: National Natural Science Foundation of China (No. 41176163); Fundamental Research Funds for the Central Universities; Comprehensive Investigation of Polar Environments (No. JDZX20110010)

First author biography: FENG Zhunzhun (1983—), male, master candidate. His research interests are remote sensing and global change. E-mail: f_zhun.whu@163.com

Corresponding author biography: CHENG Xiao (1976—), male, professor. His research interests are polar remote sensing, environment remote sensing and climate change. E-mail: xcheng@bnu.edu.cn

peated measurements of fast-changing portions of land and sea ice. IceBridge will make two major contributions to cryospheric science:

(1) Provide surface elevation data, now that the ICESat-1 mission has ended, focused on areas undergoing rapid change that are critical in characterizing selected areas of sea ice and modeling the processes that determines the mass balance of the terrestrial ice sheets. Due to the time-variable non-linear changes that these areas undergo, repeated monitoring is required. IceBridge also allows more detailed studies over these areas, though over much smaller overall areas.

(2) Support complementary measurements critical to ice models, such as bed topography, grounding line position, and ice and snow thickness. These parameters cannot be measured by satellite but can be measured from aircraft. They are the other great unknowns in understanding ice in general and developing predictive models of sea level rise in response to climate change.

Aircraft platforms utilized by the IceBridge mission include the NASA DC-8 airborne laboratory, NASA P-3B airborne laboratory, HU-25C Guardian Falcon, National Science Foundation Gulfstream V research aircraft, NASA King Air B200 airborne laboratory, UAF Otter, and many more. The on-board multiple instruments employed can be divided into five types: digital camera, lidar altimeter, radar, gravimeter, and auxiliary equipment. The main instruments are listed in Table 1.

Table 1 The main instruments employed by IceBridge

Instruments	Purpose
Digital Mapping System Camera (DMS)	Surface digital photography
Continuous Airborne Mapping By Optical Translator (CAMBOT)	Surface digital photography
Airborne Topography Mapper (ATM)	Ice surface elevation
Laser Vegetation Imaging Sensor (LVIS)	Ice surface elevation
University of Alaska Fairbanks Glacier Lidar (UAF lidar)	Ice surface elevation
Sigma Space Photon Counting Imaging Lidar (Sigma-Space Lidar)	Ice surface elevation
Ku-band radar altimeter	Ice surface elevation
Snow radar	Snow thickness
Accumulation radar	Near-surface layers
Multichannel Coherent Radar Depth Sounder (MCoRDS)	Bedrock elevation
Pathfinder Advanced Radar Ice Sounder (PARIS)	Ice inner profile
Sander/LDEO airborne gravimeter	Water depth and sub-ice geology
Bell BGM-3 gravimeter	Water depth and sub-ice geology
Position and Orientation System/Avionics 510 (POS/AV 510)	Platform position and attitude
NSERC Airborne Meteorological Instruments (AMET)	Meteorological parameters
UCAR/EOL atmospheric chemistry instruments	Atmospheric chemistry

The IceBridge mission successfully completed the 2009, 2010, and 2011 campaigns both in the Arctic and Antarctica, as shown in Fig. 1. IceBridge products can be divided into five levels. Level 0 defines the raw data, the geolocated, quality-controlled primary along-track product with artifacts removed is defined as Level 1, and Level 2 products are the geophysical variables derived at the same or similar resolution as the Level 1 source data. Most of these data products have been released by NSIDC (National Snow and Ice Data Center) ([2012-06-29] http://nsidc.org/icebridge/portal/). Level 3 data define variables mapped on uniform space-time grids, and Level 4 data define model outputs or results from analyses of lower level data. NSIDC uses polar stereographic projections for IceBridge-projected gridded data types based on the WGS-84 ellipsoid, with parameters of standard parallel 70° N and longitude of the origin 45° W for the Arctic and standard parallel 71° S and longitude of the origin 0° for Antarctica.

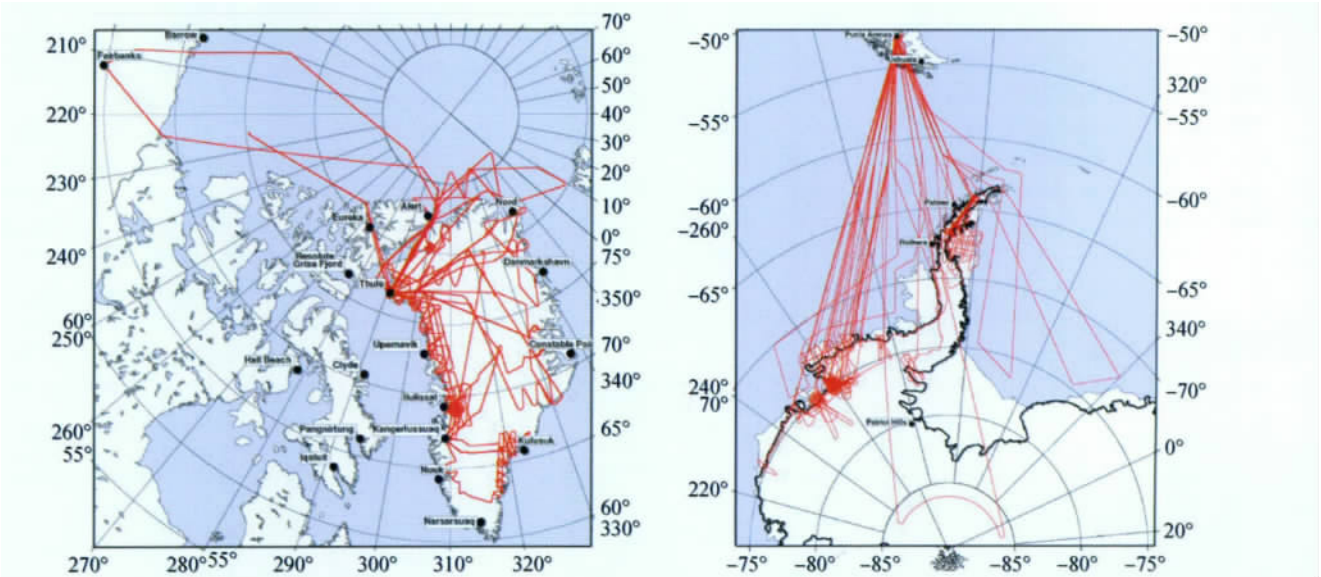

Fig. 1 A compilation of flight lines shows the paths of the 2009 Arctic and Antarctic campaigns (Koenig, et al., 2010)

3 SENSORS AND DATA PRODUCTS

3.1 Optical sensors

As a traditional means of remote sensing, optical remote sensing plays an irreplaceable role in the polar research which refers to polar geomorphology mapping, terrain classification, glacier v elocity extraction, shoreline change monitoring, and sea ice extent and distribution. Airborne optical remote sensing systems involved in the IceBridge mission are DMS and CAMBOT. DMS images with an 80% along-track overlap, combined with position and attitude data of platform, can be used for generation of high-precision photogrammetry.

3.1.1 DMS

DMS is an airborne digital camera that acquires high-resolution natural color and panchromatic imagery from low and medium altitude aircraft. The core of the system is a Canon EOS 5D Mark II digital camera that configures a Canon F1.8 28 mm lens with a 70° field of view and an R&D 36 mm × 24 mm CMOS sensor that can achieve 21.1 million effective pixels for high-quality image and 3 .9 f/s high-speed continuous shooting performance. The system is further equipped with nine auto-focus points and six invisible assist auto-focus points to capture high-speed mobile targets. The resulting image size is 5616 × 3744 pixels. The detailed photogrammetric p arameters of DMS are listed in Table 2.

Table 2 DMS photogrammetric parameters

Altitude/m	Focal Length/mm	Cross-track FOV/(°)	Along-track FOV/(°)	Nadir Pixel Resolution/m	Swath Width/m	Swath Length/m	Area/km^2
457.2	28	64.0	45.2	0.10	571	381	0.57
12192	28	64.0	45.2	2.71	15239	10160	400.81
12192	85	23.3	15.6	0.89	5020	3347	43.49

Released DMS data products include Level 0 images, which are raw data stored in JPEG format, and Level 1B images, which have been geolocated and ortho-rectified. Photogrammetric parameters have been embedded into the L1B data, which are finally stored in GeoTIFF format. These photogrammetric parameters include coordinates and projection information, the GPS date and time, pitch, roll, altitude, shutter speed, and imaging mode. These two products have been made available to users in October 16, 2009 via FTP.

3.1.2 CAMBOT

The CAMBOT system consists of a control unit, GPS, and two Kodak DC4800 digital cameras with 35 mm lens and 0.7 s exposure time. File sizes from this system can reach 3.3 million pixels at 2160 × 1440. CAMBOT operates in two modes, sequential and parallel. In sequential mode, one camera is operated at one time, giving a c ontinuous rate of one image every 10 seconds. When the compact flash card is full, the system switches to the next camera and the p revious camera begins to transfer the images to computer. In parallel mode, both cameras are used simultaneously, giving a rate of one image every five seconds. Each time CAMBOT is run, it creates two files to log the GPS and photograph information respectively. These files are then used during post-processing to correlate the i mages with the GPS data, forming geolocated Level 1B image data accompanying a text file containing the following information: time of day, latitude, longitude, altitude of aircraft above ground, ATM range, pitch of aircraft, roll of aircraft, and heading of aircraft. This information facilitates further photogrammetric data processing. R eleased data include ASCII text files for navigation data and PNG or JPEG format files for images; these have been distributed since March 31, 2009 via FTP.

3.2 Lidar sensors

Lidar instruments, the main force of data collection in the I ceBridge mission, are mainly used for surface measurements of the polar ice sheets and glaciers, which can then be used to monitor the seasonal and interannual changes in the polar mass balance, the long-term trends of the Earth surface processes, or the net mass balance between glaciers. Other applications include the measurement of sea ice height, calibration of satellite lidar, survey of sea surface height and wave characteristics, and so on. Because of the application history in the glaciology field (Krabill ,et al. , 1995), the participated ATM is a key for repeatability of the longest records. LVIS provides important coverage due to its medium and high operational altitude (Blair ,et al. , 2010). The UAF lidar is mainly used to monitor the mountain glaciers of the Alaska. Another critical point is the Sigma Space photon counting imaging lidar employed in the Investigating the Cryospheric Evolution of the Central Antarctic Plate project, which is now part of the IceBridge mission. The parameters of these four lidar instruments are listed in Table 3. As an advanced-technology application in the cryospheric field, the Sigma-Space lidar is a pathfinder for next-generation, high-efficiency, spaceflight laser a ltimeters in ICESat-2 R&D works (Krainak, et al. , 2010).

Table 3 Performance parameters of four LIDAR instruments in the IceBridge mission

Performance	ATM	LVIS	UAF	Sigma-Space
Measurement rate/Hz	5000	500—5000	10000	20000
Scan angle/(°)	±15	±12	±30	±26
Scan rate/Hz	20	10	20	20
wavelength/nm	532	1064	905	532
Pulse width/ns	—	8	—	—
Footprints size/m	1	20	0.2	—
Footprints space/m	4—7	10—20	1	horizontal: 0.15 vertical: 0.3
Swath/m	140—250	2000	500—600	400

3.2.1 ATM Lidar

ATM Lidar is one of the most important on-board instruments to execute this mission. A major task of the ATM developed by NASA since 1993 is measurement of the Greenland ice sheet with the goal of determining changes in the ice sheet elevation. After s everal improvements, the third-generation ATM used in IceBridge r emains the main lidar instrument for glacier measurements. With a designed flight altitude of ranging from 800 m to 1400 m, the ATM measures topography with an accuracy of ten centimeters by incorporating measurements from Global Positioning System (GPS) r eceivers and Inertial Navigation System attitude sensors (Krabill ,e t al. , 2002). To precisely assist ATM data acquisition using flight trajectories, NASA also developed a flight management system to further enhance the measurement accuracy of ATM. As the ATM a dopts conical scanning, its footprints form a series of ellipses with a certain overlap degree. The raw laser range data is processed to form a big-Edina (the data storage method, in which high-byte data are stored in the

low address of the memory and low-byte data are stored in the high address of the memory) binary file with a suffix of * qi. The formed Level 1 file includes GPS time, coordinates of latitude and longitude, elevation, start pulse signal strength, reflected l aser signal strength, scan azimuth, pitch, roll, GPS position dilution of precision, and laser received pulse width. At the same time, NSIDC also releases the Level 2 text format data, the contents of which include time, latitude, longitude, elevation, south to north slope of the block, ofst to east slope of the block, accuracy, number of points used and edited in estimating the aircraft parameters, and track identifier.

3.2.2 LVIS Lidar

The LVIS Lidar is a medium- and high-altitude, medium sized-footprint, all-digital waveform airborne scanning laser altimeter that is representative of the first application of waveform analysis technology in the world, designed, and developed at NASA's Goddard Space Flight Center. By sampling the entire returned pulse through a digital recorder, waveform lidar obtains the amplitude information a long with time of each returned pulse after interaction with the t errain surface and forms a more complete waveform profile. C ompared with discrete returned pulses, the waveform profile can present richer surface features and more detailed information in the vertical direction. LVIS is mainly used for precise mapping of the surface topography and measurements of the multi-scale vertical structure of ice (Hofton ,et al. , 2010), as shown in Fig. 2. A preliminary assessment of the accuracy of this instrument is 7 cm (Hofton ,et al. , 2009). Thus, comparing the multi-temporal waveform information in the same place can yield the change information of the ice surface. The LVIS data released by IceBridge team include raw data (Level 0), waveform data (Level 1B), and point-cloud data products (Level 2), the contents of which include point ID, GPS time, latitude, longitude, elevation, and the height when a pulse is 100% returned.

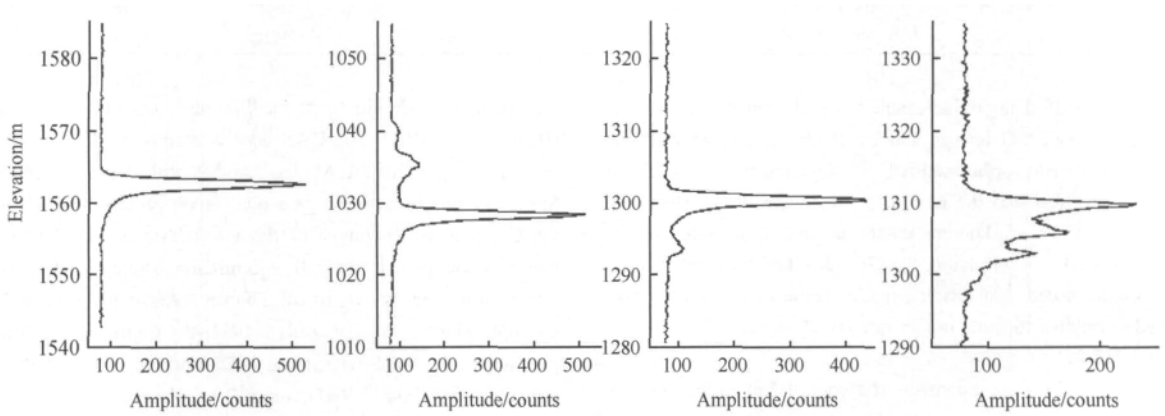

Fig. 2 Examples of lidar-returned pulse characteristics of an ice surface (Blair, et al. , 2011)

3.2.3 UAF Lidar

The UAF lidar system consists of a RIEGL LMS-Q240i scanning laser altimeter, AN Oxford technical solutions inertial, and a Trimble GPS receiver. The comprehensive accuracy of this system is in the order of 10 cm (Larsen, et al. , 2009). Since 1993, the G eophysical Institute at the University of Alaska has performed light aircraft laser altimetry surveys of over 200 glaciers across the region (Larsen ,et al. , 2010). The UAF lidar has been a part of the Ice-Bridge mission since 2009 and conducts data collection in May and August every year based on previous observations. At present, the UAF lidar data of 2009 and 2010 have been successfully acquired and released. The RIEGL laser scanner uses the pulsed time-of-flight range measurement principle and beam scanning by means of an opto-mechanical scan mechanism, providing fully linear, unidirectional, and parallel scan lines. It saves the observations in b inary format on PC machine.

UAF lidar data are post-processed to produce profile data of 25 glaciers and scanning data of 29 glaciers, which are stored in * .las format files. Each file, the contents of which include xyz coordinates in UTM projection based on the WGS84 coordinate system and return intensity, is created for one glacier in a specific time.

3.2.4 Sigma-Space Lidar

Employing a high-frequency, low-energy laser transmitter and a photomultiplier single photon detector, the Sigma-Space lidar can d etect a target by photon counting, instead of by waveform measurement, making full use of the photon energy in the returned pulse and thus greatly improving the survey efficiency of the imaging lidar. A passive diffractive optical element employed by the Sigma-Space lidar splits the transmitter beam, with about 80% efficiency, into a 10 × 10 array of 100 beamlets. Thus, each beamlet contains slightly more than 1 mW of power (about 50 nJ at 22 kHz). The returns from the 10 × 10 ground array of beamlets are directly imaged onto the photocathode of a 10 × 10 segmented anode microchannel plate p hotomultiplier. The individual anode outputs are then fed into one channel of a multichannel, multistep timing receiver with a deadtime of less than 2 ns resolution. Thus, each pulse records a 10 × 10 pixel three dimen sional volumetric image, and the individual images are continuously mosaiced together at unprecedented rates of up to 2 .2 megapixels per second (Degnan ,et al. , 2007). The single shot range accuracy of this system is roughly 6 cm (Degnan, 2010). The Sigma-Space lidar records all photon events, including signals and random background noise (such as solar noise), during the pulse transmission, so it is necessary to extract the effective data range from all records using Sigma-developed noise-editing filters, as shown in Fig. 3.

Since the green wavelength is near the peak transmission of w ater, the photon-counting lidar can detect the underlying terrain through tree canopies and thick atmospheric haze; it is also suitable for underwater imaging applications. As shown in Fig. 3, in addition to the melt pond surface observations (green dots), the bottom of melt pond observations (blue dots) is also clearly presented, thus forming a three dimen sional image of the melt pond.

3.3 Radar sensors

In order to accurately measure the mass balance of ice sheet and understand the mechanism of glacier dynamics, quantitative i

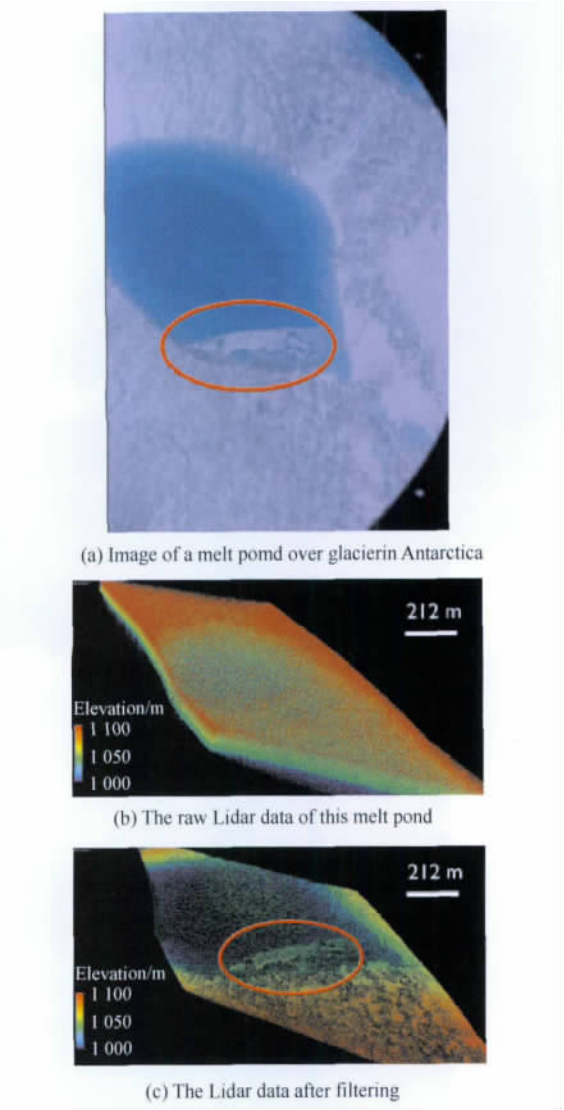

(a) Image of a melt pomd over glacierin Antarctica

(b) The raw Lidar data of this melt pond

(c) The Lidar data after filtering

Fig. 3 Image of a melt pond over glacier in Antarctica; the raw Lidar data of this melt pond and the Lidar data after filtering (Degnan, 2010)

dentification of the gas-snow-ice-bedrock geometric information and three-dimensional distribution, such as the snow accumulation, snow thickness on sea ice, ice sheet thickness, and basal geomorphic characteristics, besides the surface information acquired by lidar instruments, is necessary. Radar sensors are particularly important for this purpose. As early as 1993, the University of Kansas had developed an echo radar with an operating frequency of 150 MHz to measure the thickness of the Greenland ice sheet (Leuschen, et al., 2010). L ater, the CReSIS (Center for Remote Sensing of Ice Sheets), grouped on the basis of the University of Kansas, developed a series of different operating-frequency radar instruments with different r esolutions and snow/ice penetrating abilities. Radar sensors that are used in the IceBridge mission, including MCoRDS, accumulation r adar, snow radar, and Ku-band radar altimeter, were all developed by the CReSIS. The PARIS radar developed by Johns Hopkins U niversity is also employed in the IceBridge mission. A brief introduction of these radar instruments is given in Table 4.

3.3.1 Ku-band Radar Altimeter

Ku-band radar altimeter is a wideband radar altimeter with a center frequency of 14 GHz, pulse lengths ranging from 170 μs to 240 μs in Antarctica, a pulse length of 240 μs in Greenland, transmittance power of 20dBm, and sampling frequency of 62.5 MHz. Assuming a snow density of 0.5 g/cm^3, the range resolution of this radar can increase by up to 5.3 m in Greenland and up to 10.6 m in Antarctica. The latest research (Willatt, et al., 2011) shows that 25% and 80% of all scattering back returns come from the snow/ice interface when snow temperatures are up to −4 ℃ and −8 ℃, respectively; the rest of the returns come from air/snow interface. These results indicate that the Ku-band radar penetrates further into the snow cover at lower temperatures. Thus, differences in elevation between Ku-band radar and laser altimeters could represent the snow depth o ver sea ice. Observations reveal that Ku-band radar can penetrate into the near-surface firn of ice sheet with a depth of 15 m and into the snow on sea ice with a depth of 0.5 m (Patel, et al., 2010). After the processing of pulse compression, including coherent integration, high-pass filtering, noise removal, and height correction (Blake, 2010), the raw radar data is stored in * .bin format files, the contents of which include time, latitude, longitude, height, return time of s urface and bedrock, and intensity. A JPEG file stores snow/ice echogram images along the flight paths.

Table 4 Radar instruments adopted in the IceBridge mission

Instrument	Measurement	Frequency (bandwidth)
MCoRDS	Ice thickness Bed imaging Internal layering	195 MHz (30 MHz)
Accumulation radar	Internal layering	750 MHz (300 MHz)
Snow radar	Snow cover Internal layering Topography	4.5 GHz (4 GHz)
Ku-Band radar altimeter	Snow cover Topography	14 GHz (4 GHz)
PARIS	Internal layering Topography	150 MHz (6 MHz)

3.3.2 Accumulation Radar

Accumulation radar is designed to map the variation of snow accumulation rate. When installed on aircraft, it operates at a f requency of 750 MHz with a bandwidth of 300 MHz, providing 28 cm depth resolutions in ice. Other characteristics of this radar include a scan duration of 10 ms, transmittance power of 100 mW, Yagi a ntennae for both the transmitter and receiver, sampling frequency of 5 0 MHz, and 12 bit analog or digital converter for signal processing. The data files are in binary format and associated GPS files are p rovided in MATLAB and Applanix output formats. JPEG image files and KML files are also included. The data products have been available for periodic operation since May 2010 via FTP.

3.3.3 Snow Radar

Snow radar is an ultra-wideband radar developed by the CReSIS with a frequency of 4.5 GHz, a pulse width of 250 μs, a repetition of 2 kHz, a transmission power of 20 dBm, and a sampling frequency of 60 MHz. Assuming a snow density of 0.3 g/cm^3, the range resolution of this radar may be as high as 2.5 m in Greenland measurements and 5.25 m in Antarctic measurements. It is designed to map near-surface internal layers in polar firn with fine vertical resolution, as shown in Fig. 4. Knowledge of snow thickness is essential to the estimate mass balance and surface energy exchange of sea ice. The radar is also used to measure snow thickness and distribution over sea ice (Kowk, et al., 2010). The collected data is stored in * .bin format files, the contents of which include time, latitude, longitude, height, return time of surface and bedrock, and i ntensity. A JPEG

file is also given, showing the snow or ice echogram images along the flight paths.

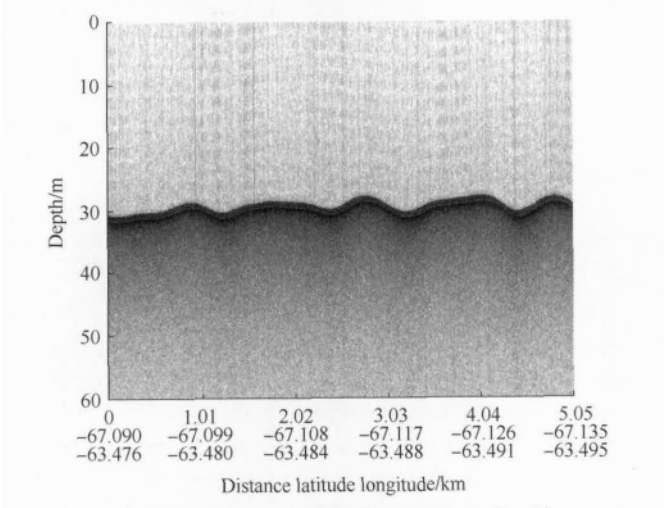

Fig. 4 Snow echogram of Pine Island area produced by snow radar (Leuschen & Carl, 2011b)

3.3.4 MCoRDS

MCoRDS, developed by the CReSIS, operates at a frequency of 195 MHz with multiple receivers developed for airborne sound and imaging of ice sheets. The radar bandwidth is adjustable and its vertical range resolution can reach 4.2 m. Multiple receivers permit digital beam steering to suppress cross-track surface clutter than can mask weak ice-bed echoes and strip-map synthetic aperture radar images of ice-bed interfaces (Lohoefener, 2007). Five of the eight radar channels used were set up to capture surface or bed echoes and ice thickness (radar channels). The remaining three channels are connected to antennas within the cabin of the plane and were operated in receiving mode only to measure electromagnetic interference (EMI) channels. EMI channels can pick up most of the surface returns, even in areas where radar channels cannot. Therefore, data derived from EMI channels may be used in many cases for ice thickness estimations. Ice thickness is typically determined using data collected from waveforms with different durations and different receiver channels. The difference in times-of-arrival between ice and bed signals is then converted into ice thickness.

IceBridge provides MCoRDS L1B geolocated radar echo strength profile data, L2 ice thickness data, L3 gridded ice thickness, and surface and bottom data. The L1B data include measurements for echograms, time, latitude, longitude, elevation, and surface, flight path charts, and echogram images. The data are stored in MATLAB files with associated PDF, TIFF, and PNG files, as shown in Fig. 5. L2 data include measurements for elevation, surface, bottom, and thickness. The data are stored in Comma Separated Value (CSV) text format with associated KML files. L3 products include flight lines, boundaries, grids, preview images, and crossover analysis. These data are collected as part of the IceBridge funded campaigns and stored in Comma Separated Value (CSV), Portable Network Graphics (PNG), Tag Image File Format (TIFF), Tiff World File (TFW), and ArcGIS shape files.

3.3.5 PARIS

The PARIS radar developed by Johns Hopkins University withan operating frequency of 150 MHz enables the visibility of internal layering and bottom topography of ice sheets when probed by high-altitude aircraft (even from spacecraft) (Raney, et al., 2008). This

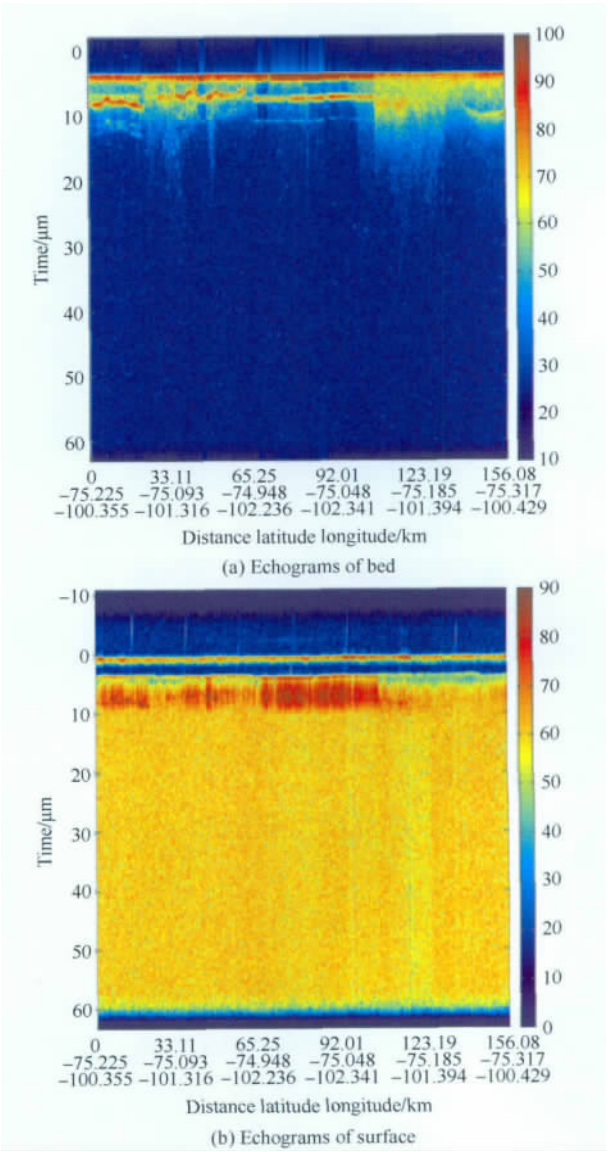

Fig. 5 Echograms of bed and surface in Pine Island area acquired by MCoRDS

radar is composed of three parts: a direct digital synthesizer, which is in charge of the synthesis and emission of the pulse; an analog to digital converter, which is in charge of receiving and converting signals from the antenna; and a field programmable gate array, which is in charge of signal processing and storage.

The signals received by the PARIS radar include not only signals from the surface return, its side lobes, and bottom returns but also signals from internal clutter, triple-bounce from aircraft to surface, along-track, and across-track clutter sources, among others. Researchers from Johns Hopkins University can effectively remove most of the above noise using partially coherent Doppler processing, as shown in Fig. 6. The resulting data files are in ASCII text format and contain fields for latitude, longitude, time, ice thickness, aircraft altitude, and confidence of thickness measurement, which has five grades ranging from 1 to 5, corresponding to data quality from good to bad.

3.4 Airborne gravimeter

Gravity data can be used to map and interpret features hidden

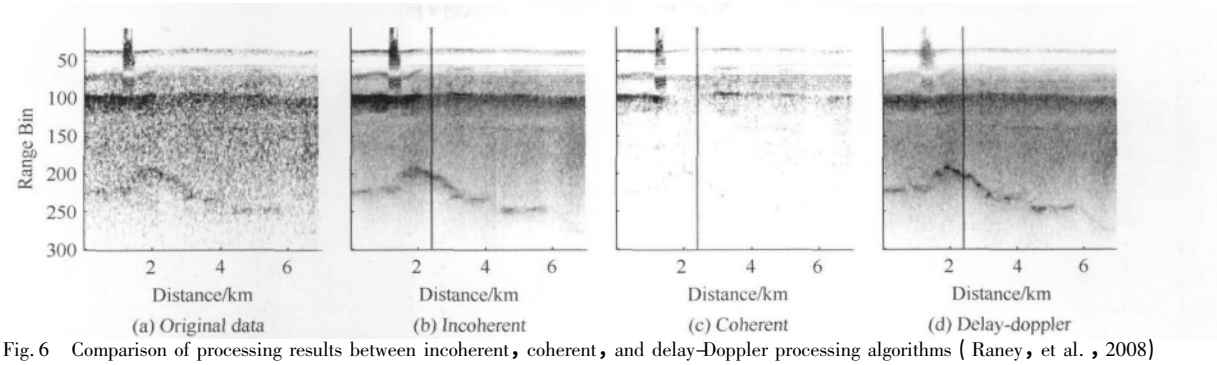

Fig. 6 Comparison of processing results between incoherent, coherent, and delay-Doppler processing algorithms (Raney, et al., 2008)

by snow and ice in polar regions, especially those related to volcanoes, faults, water, and even tectonic events. Instruments mounted on aircraft flying over the glaciers can use lasers to measure the ice surface and radar by penetrating through the ice to map topography and cavities underneath or in the ice. However, the amount of water existing underneath the ice is unknown. Knowledge of this information is key in assessing the impact of water on dynamic changes in the entire icesheet. Newly refined high-resolution gravity technology must be used to assess the influence mechanisms of the water under ice (Studinger, et al., 2010). The IceBridge mission expands the use of the airborne gravimeter. Aside from bathymetry, it also allows Fjord geophysical prospects, assists in ice thickness measurements, and helps assess the impact of warm sea water on acceleration of the melting of the ice shelf basal (Cochran, et al., 2010). Key areas surveyed by gravimeters include the Peterman, Zachariae, Jakobshavn, and Russell Glacier areas in Greenland and the Abbot Ice shelf, Larson Ice shelf, Antarctic Peninsula, Pine Island glacier, and Thwaites Glacier areas in Antarctica.

The gravimeter system employed by the IceBridge mission is the AIRGrav system developed by Sander Geophysics Limited; it is the only purpose-built airborne gravimeter designed primarily for petroleum exploration. The AIRGrav system uses three orthogonal accelerometers as gravity sensors on a three-axis gyroscopically stabilized platform, combined with a high resolution differential GPS to correct for aircraft movements caused by turbulence, aircraft vibrations, and drape flying, guaranteeing the flight horizontal error within 10 rad/s. High precision differential GPS processing techniques and a robust gravimeter system have resulted in final processed gravity grids with noise estimates of 0.3 mGal at a resolution ranging from 2.2 km to 4 km (Sander, et al., 2004). AIRGrav data consist of aircraft attitude and gravitational measurements. Aircraft attitude is provided as one file per flight. Gravity data are divided into one file for each geographic area, plus an additional file containing all remaining transit lines, lines that do not fall within one of the grids, lines within a grid that cross at significantly different altitude, and lines within a grid that are contaminated by maneuver noise and could be dropped in favor of other lines, as shown in Fig. 7. Gravity data include time, coordinates, latitude and Etovos corrected values, and the free air correction at various along-flight-line spatial filtering scales. The formula for calculating free air gravity anomalies using the above gravity values is as below.

$$FAA = A_{\text{measured}} - A_{\text{aircraft}} + Eotvo + FAC - G_{\text{the}}$$

where FAA is the free air anomaly, A_{measured} is the measured gravity, A_{aircraft} is the aircraft acceleration, $Eotvo$ is the Bouguer correction; FAC is the free air correction, and G_{the} is the normal gravity.

The BGM-3 gravimeter, developed by Bell Aerospace and employed by ICEAP project, was primarily designed for ship-borne measurement and specially upgraded to suit airborne environments. The BGM-3 system consists of a forced feedback accelerometer with a recording rate of 1 Hz and a detection range of 30 G mounted on a gyrostabilized platform. Combined with GPS measurements, the accuracy of this system can be up to 1 mGal (Richter, et al., 2002). In the IceBridge operation, the BGM-3 system is used for gravity surveys of the southeastern Antarctic region. The BGM-3 products of L0 raw accelerations, L1B time-tagged accelerations, and L2 geolocated free air anomalies are stored in ASCII format and available for periodic and ongoing campaigns from 2009 to the present via FTP.

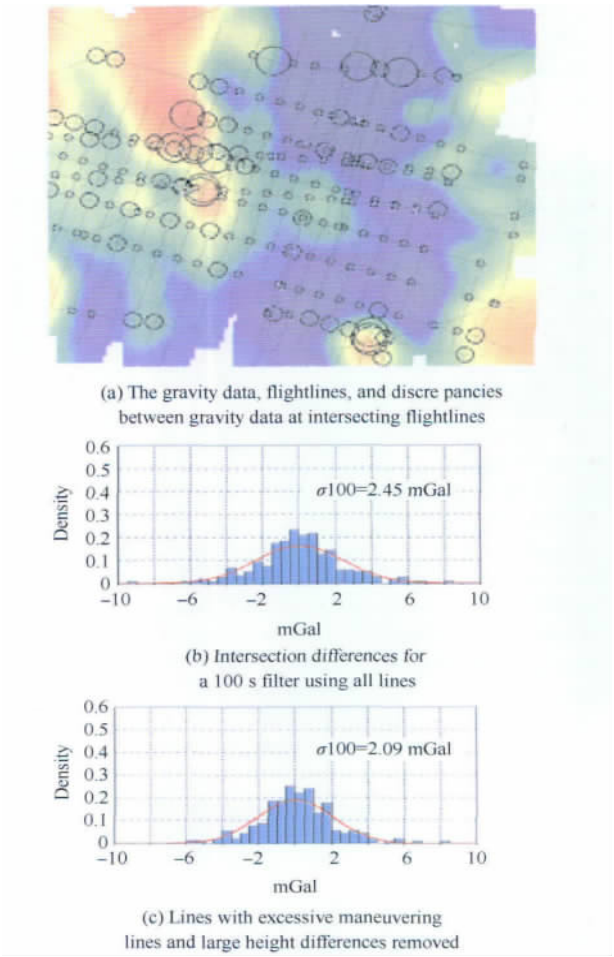

Fig. 7 The gravity data, flightlines, and discrepancies between gravity data at intersecting flightlines (the circle sizes represent mismatches) in the Pine Island area. Intersection differences for a 100 s filter using all lines and lines with excessive maneuvering lines and large height differences removed (Cochran, et al., 2011)

3.5 Auxiliary equipment

3.5.1 POS/AV 510

Almost all on-board observations are influenced by the platform's position and orientation, so high-precision position and orientation information is a basic guarantee of the measurement of an entire project. The IceBridge operation employed the Canada POS/AV 510 to correct the airborne platform's trajectories. By integrating Global Navigation Satellite System with an inertial measurement unit, the world's most advanced POS system can have an absolute positioning accuracy of 5 cm, roll and pitch accuracy of 0.005°, and true heading accuracy of 0.008° (Mostafa & Hutton, 2002). The collected data in the way of coupling POS/AV with DMS, when operated, can be applied to all on-board instruments. The released L1B data parameters include time, latitude, longitude, altitude, velocity, roll, pitch, and heading.

3.5.2 National Suborbital Education and Research Center (NSERC) Airborne Meteorological Instruments

The IceBridge mission employs airborne meteorological instruments provided by the NSERC. The collected data set contains 36 parameters of airborne in-flight meteorological and in-cabin measurements and thermal emission measurements of near-nadir surface skin temperature, including solar zenith angle, air temperature, air pressure, humidity, wind speed, infrared surface temperature, soil temperature, cabin pressure, and instrument temperature, among others. Instruments used for the collection of meteorological data include the following: an MKS Baratron type 220D pressure transducer, a two-stage Buck research hygrometer, a three-stage Edgetech model 137 hygrometer, a total air temperature Goodrich model 102, and a Heritronics infrared radiation pyrometer. Data are taken at 1 Hz from aircraft and facility instruments on-board and then recorded on two redundant NASA airborne science data acquisition and transmission flight recorders. After export, conversion, and quality control, data are stored in an Intercontinental Chemical Transport Experiment (ICARTT) comma separated format. These data have been made available for periodic and ongoing campaigns since 12 October 2009 via FTP.

3.5.3 National Center for Atmospheric Research/Earth Observing Laboratory (UCAR/EOL) Atmospheric Chemistry Instruments

Aside from meteorological parameters, atmospheric chemistry parameters, which are closely related to climate change, are also measured in the IceBridge mission by the UCAR/EOL using an AVOCET differential non-dispersive infrared gas analyzer instrument, an airborne differential absorption CO measuring instrument, a diode laser hygrometer, and airborne whole air samplers. The data set includes measurements for CO_2, CO, CH_4, N_2O, H_2O (v), and whole air samplers. The data are stored in ICARTT format and were available from 12 October 2009 to 24 November 2009.

4 APPLICATIONS OF THE ICEBRIDGE OBSERVATION DATA

As the largest airborne survey of the Earth's polar ice ever known, the IceBridge mission will establish a series of long-time observations of the change characteristics of the polar ice sheets and sea ice, combined with ICESat-1/Cryosat-2/ICESat-2. It will also focus on the polar areas undergoing rapid change in order to understand the ice in general and develop predictive models of sea level rising. Prospects of research based on IceBridge data may be given in terms of four aspects.

4.1 Three-dimensional mapping of snow/ice

Instruments on board the IceBridge mission have provided favorable conditions for detecting the material composition and distribution of polar regions in all dimensions and multi-perspectives. Using lidar data, optical images can acquire information of a surface's land cover and topography. Radar sensors are used to detect internal ice layering and bed characteristics beneath the ice. Gravitational observations provide geometric parameters of sub-ice features, such as cavities, subglacial lakes, and troughs (Griggs & Bamber, 2010; Hofton, et al., 2010; Richter, et al., 2002; Studinger, et al., 2010). Therefore, observations acquired by all of the instruments provide an exceptional foundation for polar research. Fig. 8 shows a three dimensional mapping of Pine Island glacier with the surface elevation determined from ATM over a Radarsat-1 SAR image, lower ice surface determined from MCoRDS radar, ice velocity (yellow arrows) extracted from Radarsat-1 data, and the grounding line (purple line). The figure illustrates a deep trough upstream of the glacier tongue and the distributions of iceshelf thickness and several tributary glaciers. Qualitatively, surface velocity directions are consistent with subglacial topography, suggesting that flow divergence with depth may be small.

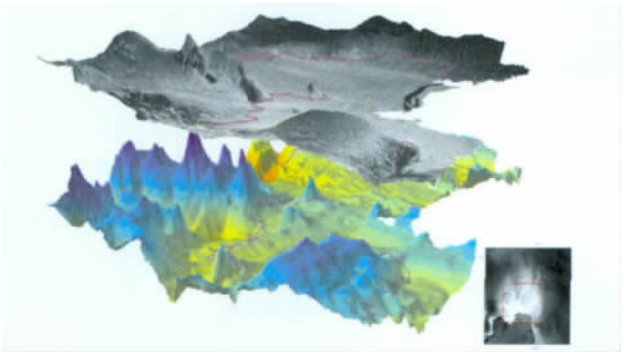

Fig. 8 Three dimensional mapping of Pine Island glacier, Antarctica (Blake, et al., 2010)

A three-dimensional high-definition map of a crevasse in the Thwaites iceshelf may be illustrated by combining lidar and DMS data, as shown in Fig. 9.

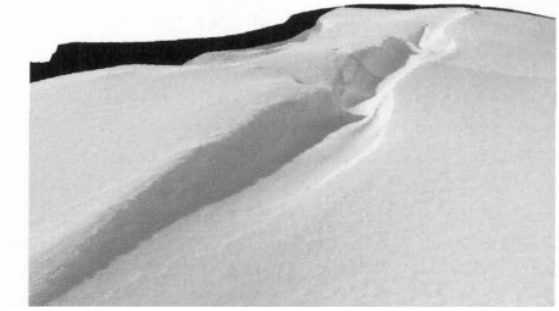

Fig. 9 Three dimensional mapping of a crevasse in the Thwaites iceshelf, Antarctica

Scientists have recently begun to pay more attention to the mapping of bedrock terrains below the icesheet using gravity anomaly data and made considerable achievements in this field. Tinto and Bell (2011) identified a prominent ridge with two distinct peaks 40 km in front of the present-day grounding line using a new bathymetric model

from the Thwaites glacier region based on I ceBridge airborne gravity data and pointed out that these features exert key controls in the evolution of ice flow. Cochran and Bell (2012) produced an inversion of the IceBridge gravitational data for continental shelf bathymetry beneath the Larsen ice shelf, successfully showing ocean water troughs and water-filled cavities. Shodlok, et al. (2012) found that the temporal variability of melting in the Pine Island ice shelf is mostly driven by the processes of warm circumpolar deep water outside the cavity and that the simulated mean melting rate is 28 ma^{-1} according to NASA IceBridge data, much higher than previous model estimations but close to remote sensing findings.

4.2 Glacier elevation and mass balance estimation

Changes in the elevation of polar glaciers are the most intuitive factors in global change research, the main principle of which involves the use of elevation differences in height observations at different times but the same regions to calculate the ice mass balance using the integral method combined with the distribution of ice and snow density. Altimeter sensors on board the IceBridge mission play a great role in this undertaking (Sonntag & Krabill, 2009). Since 1993, UAF scientists have used laser altimetry systems to measure surface elevation changes in over 200 glaciers throughout Alaska and western Canada every three of five years. In the 2009 IceBridge campaign, 40 glaciers were re-measured. Analysis of these survey data led to the discovery that the melting rate of most glaciers twice or more than that five to ten years ago (Larsen ,et al., 2009), as shown in Fig. 10. The latest research shows that the mass balance of Alaska glaciers is $-41.9\ km^3 \pm 8.6\ km^3$, contributing 0.12 mm ± 0.02 mm to the sea level rise (Berthier ,et al., 2010).

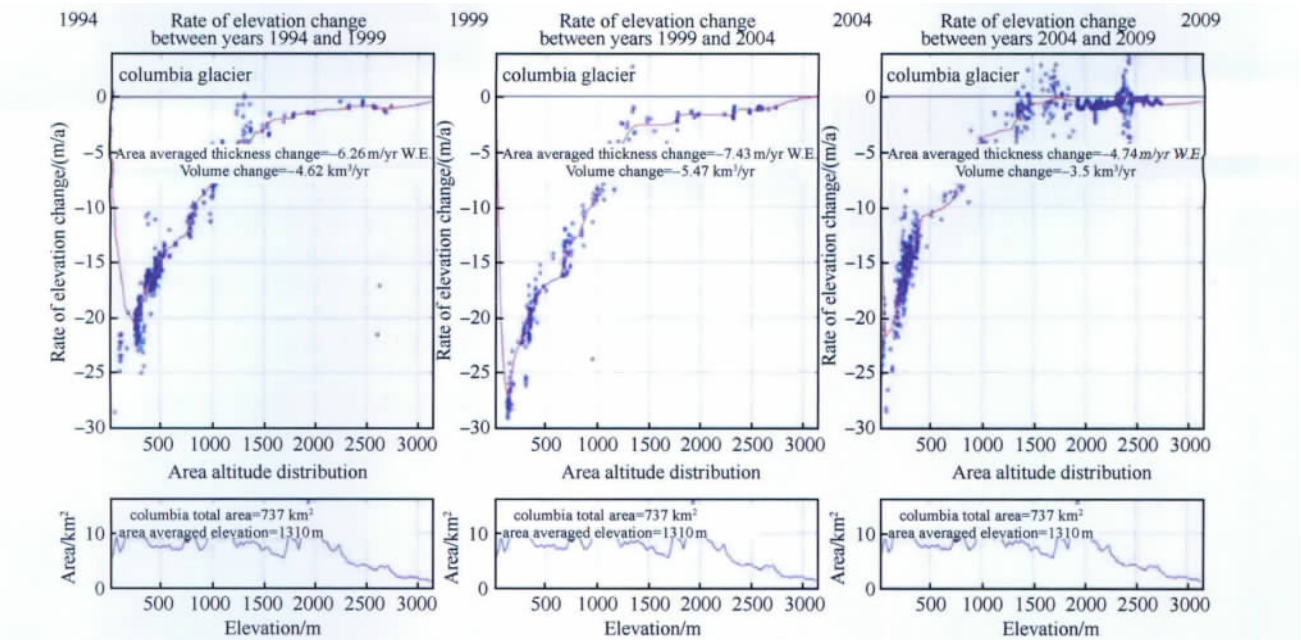

Fig.10 The rate of elevation change and elevation-area from 1994 to 2009 of Columbia Glacier in the Alaskan region (Larsen, et al., 2009)

Gravitational anomaly differences acquired by a gravimeter across the same region can also be used to directly calculate the mass balance using the integral method. The availability of multi-sensor observations of glaciers provided by the IceBridge mission makes the calculation of mass balance by fluxes method possible. For example, new radar ice thickness data can constrain glacier ice mass fluxes; bathymetry data and the distribution of cavity underneath ice shelves derived from an airborne gravimeter can help estimate water fluxes associated with the interaction between i ce-shelf and ocean, and, snow depth and firn layering data can be used to estimate accumulation rates. However, significant gaps remain in some parts of Greenland, which is not covered by radio echo sounding, and Antarctica. IceBridge collects ice thickness data along the Bellingshausen Sea sector, where hardly any data had been collected in the past. Thus, calculating mass balances must be done by the flux method using other satellite data and climate-sea-ice sheet models (Rignot, et al., 2010).

4.3 Spatio-temporal changes in sea ice thickness and extent

Sea ice is particularly sensitive to climate change; thus, the study of sea ice changes in polar regions is extremely important. The extent and thickness dynamics of sea ice extracted from DMS, radar, and lidar data can not only help researchers understand sea ice physics but also allows analysis of its evolutionary process in current c limate patterns. Sea ice thickness can be inferred from two quantities, namely, the freeboard portion of the sea ice and the snow depth, a ssuming hydrostatic equilibrium, i. e. (Kurtz, et al., 2008),

$$H_f = H_{si} - H_{ss} = h_s + f_b$$

$$h_i = \frac{\rho_s}{\rho_w - \rho_i} h_s + \frac{\rho_w}{\rho_w - \rho_i} f_b$$

where ρ_i, ρ_s and ρ_w are the densities of the snow, sea ice, and water, respectively, h_i is the sea ice thickness, H_{si} is the sea ice surface elevation acquired by ATM lidar, H_{ss} is the sea surface elevation, which can be derived from gravity data, h_s is the snow thickness over sea ice, which can be acquired by Ku-band radar or snow radar, and f_b is the sea ice freeboard.

4.4 Calibration and validation to satellite remote sensing observations

The IceBridge mission will annually collect sea ice and ice sheet data 30000 km along the ICESat-1 satellite orbit and at least 500 km along the CryoSat-2 orbit. This mission will not only bridge the obser-

vation gap between ICESat-1 and ICESat-2, establish a series of long-time elevation observations, and provide data for calibration and validation of laser satellites (ICESat-1, ICESat-2) and r adar satellites (CryoSat-2, Envisat) but also carry instruments for the simulation and performance evaluation of the new ICESat-2 and DesDynI-Lidar. In the Envisat/RA-2 altimeter validation mission of 2006, good overall consistency between RA-2 and ATM (equipped on NASA's P-3 aircraft) elevations was obtained. The observed mean elevation difference of 36 cm was considered to be from snow accumulation over floe ice; over refrozen lead surfaces, only negligible snow accumulation and a mean difference in the order of 1 cm were observed (Connor, et al., 2009). In the 2010 IceBridge Arctic campaign, the CryoSat-2 orbit was under-flown by a NASA DC-8 a ircraft that carried a digital camera, a lidar, and radar instruments to conduct validation activities, as shown in Fig. 11 (Connor, et al., 2010).

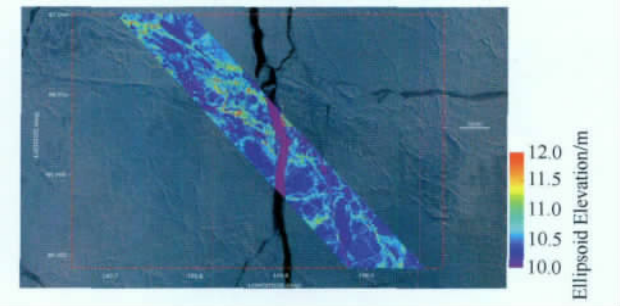

Fig. 11 ATM and Cambot observations over sea ice along the CryoSat-2 track on April 20, 2010

Airborne remote sensing observations are of high accuracy and resolution while satellite remote sensing has unparalleled advantages in wide-range coverage. Cross-validation between these methods will undoubtedly greatly expand the application of IceBridge data, although errors and uncertainties in these calibrations and verifications caused by surface type, platform noise, and inconsistent coverage are also known to occur (Connor, et al., 2009). Loss of ground validation is another factor that may bring about data uncertainties. Thus, future research will focus on establishing error sources of aerospace/airborne observations, development of calibration and cross-validation methods for satellite data, and improving the relevant algorithms using IceBridge data, which are also the premise and key for joint applications in satellite observations and airborne observations (Luthcke, et al., 2010).

5 DISCUSSION AND CONCLUSIONS

The IceBridge will not only ensure the continuity of satellite observations, but also monitor polar elements in all dimensions and perspectives by on-board instruments, significantly contributing to the understanding of the change mechanisms in polar regions. Prospects of the mission's application are very attractive to the polar research community. Comprehensive application of multi-source airborne observations, including multi-source data fusion technologies at different scales and urgent assessment and exploration of the potential application of these observations, has become an issue of concern to many scientists. Further development of polar-related models (such as ice sheet dynamics, glacier dynamics, sea level rise, and sea ice coverage models) requires information on bedrock topography, ice thickness and structure, bathymetry underneath the ice shelf and ice tongue, snow depth and structure, and so on, which may be derived from IceBridge multi-source observations.

Despite its favorable prospects, however, the IceBridge mission has several shortcomings. Due to the limitation of aviation logistical support capacity, the present flying areas are limited to southwest Antarctica, Antarctic Peninsula regions, and western edge regions of Greenland in the Arctic. In addition, observations are often influenced by harsh polar weather conditions. Airborne remote sensing measurements have inconsistent scales and do not meet the requirements of traditional survey engineering, thereby increasing the difficulty of data post-processing.

Since 1984, the Chinese Antarctic Scientific Expedition has mainly concentrated on two regions, the Antarctic Peninsula near the Great Wall station and the Amery ice shelf near the Larsemann hills. Polar observations are mainly based on the platform of "one ship and three stations" (i. e., a Xuelong ship and the Great Wall, Zhongshan, Kunlun stations). China is now constructing a polar airborne platform that will also include remote sensing capability. The free sharing of IceBridge data will not only provide massive amounts of observational data to Chinese scientists for study but also provide technical references for the construction of China's polar aircraft r emote sensing platform.

In summary, IceBridge airborne observations can monitor dynamic changes in the ice sheet, detect the change physics of ice shelves and sea ice, and provide input and validation data for various Earth system models. The IceBridge mission not only provides a valuable data resource for the research of multi-source observational applications but also significantly aids in the understanding of the basic facts and laws of global change.

Acknowledgements: We would like to thank NASA of the USA for providing the IceBridge observations and Dr. Chi Zhaohui of Texas A&M University for helping us download the IceBridge data.

REFERENCES

Berthier E, Schiefer E, Clarke G K C, Menounos B and Rémy F. 2010. Contribution of Alaskan glaciers to sea-level rise derived from satellite imagery. Nature Geoscience, 3(2), 92 – 95

Blair J B, Hofton M A and Rabine D L. 2010. Large-area Ice Sheet and Sea Ice mapping from High-altitude Aircraft: Examples from the LVIS Sensor // American Geophysical Union, Fall Meeting 2010, abstract #C53A – 08, 08

Blake W A. 2010. Interferometric Synthetic Aperture Radar (InSAR) for Fine-Resolution Basal Ice sSheet Imaging. Lawrence: The University of Kansas

Blake W, Shi L, Meisel J, Allen C and Gogineni P. 2010. Airborne 3D basal DEM and ice thickness map of Pine Island Glacier. IEEE International Geoscience and Remote Sensing Symposium (IGARSS), 2010: 2503 – 2506 [DOI: 10.1109/IGARSS.2010.5653924]

Cochran J R, Bell R E, Frearson N and Elieff S. 2010. Inversion of IceBridge gravity data for continental shelf bathymetry beneath the Larsen ice shelf // American Geophysical Union, Fall Meeting 2010, abstract #C14A – 05, 05

Cochran J R and Bell R E. 2011. IceBridge Sander Air GRAV L1B Geolocated Free Air Gravity Anomalies. ed. IceBridge. Boulder, Colorado USA: National Snow and Ice Data Center (NSIDC)

Cochran J R and Bell R E. 2012. Inversion of IceBridge gravity data for continental shelf bathymetry beneath the Larsen ice shelf, Antarctica. Journal of Geodynamics, 58(209): 540 – 552 [DOI: 10.3189/2012JoG11J033]

Connor L N, Laxon S W, Ridout A L, Krabill W B and McAdoo D C. 2009. Comparison of Envisat radar and airborne laser altimeter measurements over Arctic sea ice. Remote Sensing of Environment, 113(3), 563 – 570 [DOI: 10.1016/j.rse.2008.10.015]

Connor L N, Laxon S, McAdoo D C, Farrell S L, Ridout A, Cullen R, Francis R, Studinger M, Krabill W B and Sonntag J G. 2010. A first comparison of CryoSat-2 and ICEBridge altimetry from April 20, 2010 over Arctic Sea Ice // American Geophysical Union, Fall Meeting 2010, abstract #C41A-0506, 0506

Degnan J J, Wells D, Machan R and Leventhal E. 2007. Second generation airborne 3D imaging lidars based on photon counting // Advanced Photon Counting Techniques II, 67710N. Boston, MA, USA

Degnan J J. 2010. Photon Counting Lidars for Airborne and Spaceborne Topographic Mapping // Applications of Lasers for Sensing and Free Space Communications (LSC). San Diego, California: Optical Society of America

Griggs J and Bamber J. 2010. A new, multi-resolution bedrock elevation map of the Greenland ice sheet // American Geophysical Union, Fall Meeting 2010, abstract #C22B-07, 07

Hofton M A, Luthcke S B, Blair J B, Rabine D and McIntosh C. 2009. Precise and Accurate High-Altitude Waveform Lidar Mapping of Greenland Land and Arctic Sea Ice in Support of Operation I ceBridge // American Geophysical Union, Fall Meeting 2009, a bstract # C51B-0488, 0488

Hofton M A, Blair B, Luthcke S, Rabine D, McIntosh C and Beckley M. 2010. Characterizing Ice Sheet Surface Topography and Structure Using High-Altitude Waveform Airborne Laser Altimetry // American Geophysical Union, Fall Meeting 2010, abstract #C11A-0523, 0523

Koenig L, Martin S, Studinger M and Sonntag J. 2010. Polar airborne observations fill gap in satellite data. Eos Transactions American Gerophysical Union, 91(38): 333-334 [DOI: 10.1029/2010EO380002]

Krabill W B, Thomas R H, Martin C F, Swift R N and Frederick E B. 1995. Accuracy of airborne laser altimetry over the Greenland ice sheet. International Journal of Remote Sensing, 16(7): 1211-1222 [DOI: 10.1080/0143116950895447 2]

Krabill W B, Abdalati W, Frederick E B, Manizade S S, Martin C F, Sonntag J G, Swift R N, Thomas R H and Yungel J G. 2002. Aircraft laser altimetry measurement of elevation changes of the Greenland ice sheet: Technique and accuracy assessment. Journal of Geodynamics, 34 (3-4), 357-376 [DOI: 10.1016/S0264-3707(02)00040-6]

Krabill W B. 2011. IceBridge ATM L1B Qfit Elevation and Return Strength. IceBridge. Boulder, Colorado USA: National Snow and Ice Data Center (NSIDC)

Krainak M A, Yu A W, Yang G M, Li S X and Sun X L. 2010. Photon-counting detectors for space-based laser receivers // Razeghi M, Sudharsanan R and Brown G J. Proceedings of the SPIE 7608, 760827. San Francisco, California, USA

Kurtz N T, Markus T, Cavalieri D J, Krabill W, Sonntag J G and Miller J. 2008. Comparison of ICESat data with airborne laser altimeter measurements over Arctic sea ice. IEEE Transactions on Geoscience and Remote Sensing, 46(7): 1913-1924 [DOI: 10.1109/TGRS.2008.916639]

Kwok R, Leuschen C, Panzer B, Patel A, Kurtz N T, Markus T, Holt B and Gogineni P S. 2010. Radar surveys of snow depth over Arctic sea ice during Operation IceBridge // American Geophysical Union, Fall Meeting 2010, abstract #C21D-02, 02

Larsen C, Hock R, Arendt A and Zirnheld S. 2009. Airborne Laser Altimetry Measurements of Glacier Wastage in Alaska and NW Canada // American Geophysical Union, Fall Meeting 2009, abstract #C23C-0508, 0508

Larsen C F, Johnson A, Zirnheld S L and Claus P. 2010. Operation IceBridge Alaska // American Geophysical Union, Fall Meeting 2010, abstract #C22B-08, 08

Leuschen and Carl. 2011a. IceBridge Accumulation Radar L1B Geolocated Radar Echo Strength Profiles. Boulder, Colorado USA: National Snow and Ice Data Center

Leuschen and Carl. 2011b. IceBridge Snow Radar L1B Geolocated Radar Echo Strength Profiles. Boulder, Colorado USA: National Snow and Ice Data Center

Leuschen C, Gogineni P S, Allen C, Paden J D, Hale R, Rodriguez-Morales F, Harish A, Seguin S, Arnold E, Blake W, Byers K, Crowe R, Lewis C, Panzer B, Patel A and Shi L. 2010. The CReSIS Radar Suite for Measurements of the Ice Sheets and Sea Ice during Operation Ice Bridge // American Geophysical Union, Fall Meeting 2010, abstract #C44A-02, 02

Lohoefener A. 2007. Design and Development of a Multi-Channel Radar Depth Sounder. Lawrence: The University of Kansas

Luthcke S B, Rowlands D D, McCarthy J, Sabaka T J, Arendt A A, Loomis B and Boy J. 2010. Changes in Land Ice from GRACE: Signal, Errors and Relation to Other Missions // American Geophysical Union, Fall Meeting 2010, abstract #C43F-08, 08

Mostafa M M R and Hutton J. 2002. Direct positioning and orientation systems: How do they work? What is the attainable accuracy. International Archives of Photogrammetry and Remote Sensing, 33

Panzer B, Leuschen C, Blake W, Crowe R, Patel A, Gogineni P S and Markus T. 2010. Wideband radar for airborne measurements of snow thickness on sea ice // American Geophysical Union, Fall Meeting 2010, abstract #C21D-01, 01

Patel A, Gogineni P, Leuschen C, Rodriguez-Morales F and Panzer B. 2010. An Ultra Wide-Band Radar Altimeter for Ice Sheet Surface Elevation and Snow Cover Over Sea Ice Measurement // American Geophysical Union, Fall Meeting 2010, abstract # C41A-0518, 0518

Raney R K, Leuschen C and Jose M. 2008. Pathfinder Advanced Radar Ice Sounder: PARIS // Geoscience and Remote Sensing Symposium, III-346-III-349. Boston, MA: IEEE

Richter T G, Kempf S D, Holt J W, Morse D L, Blankenship D D and Peters M E. 2002. Airborne gravimetry and laser altimetry over Lake Vostok, East Antarctica // American Geophysical Union, Spring Meeting 2002, abstract #B22A-04, 04

Rignot E J, Schodlok M, Menemenlis D, Studinger M, Cochran J R and Bell R E. 2010. Improvements in the determination of ice sheet mass fluxes and freshwater fluxes using Icebridge data // American Geophysical Union, Fall Meeting 2010, abstract #C22B-01, 01

Sander S, Argyle M, Elieff S, Ferguson S, Lavoie V and Sander L. 2004. The AIRGrav airborne gravity system // The ASEG-PESA airborne gravity 2004 workshop: Geoscience Australia Record, 49-54

Schodlok M P, Menemenlis D, Rignot E, Studinger M. 2012. Sensigivity of ice-shelf/ocean system to the sub-ice-shelf cavity shape measured by NASA IceBridge in Pine Island Glacier, West Antarcitca. Annals of Glaciology, 53(60): 156-162 [DOI: 10.3189/2012AoG60A073]

Sonntag J and Krabill W. 2009. Recent Changes in the Periphery of the Greenland Ice Sheet from NASA's Airborne Topographic Mapper // American Geophysical Union, Fall Meeting 2009, abstract #C43D-05, 05

Studinger M, Allen C, Blake W, Shi L, Elieff S, Krabill W B, Sonntag J G, Martin S, Dutrieux P, Jenkins A and Bell R E. 2010. Mapping Pine Island Glacier's Sub-ice Cavity with Airborne Gravimetry // A merican Geophysical Union, Fall Meeting 2010, abstract # C11A-0528, 0528

Tinto K J and Bell R E. 2011. Progressive unpinning of Thwaites Glacier from newly identified offshore ridge: Constraints from aerogravity. Geophysical Research Letters, 38: L20503 [DOI: 10.1029/2011GL049026]

Willatt R, Laxon S., Giles K, Cullen R, Haas C and Helm V. 2011. Ku-band radar penetration into snow cover on Arctic sea ice using airborne data. Annals of Glaciology, 52(57): 197-205

Xu Guanhua, GongPeng, Shao Liqin, LinHai, Dai Yongjiu, Wang Bin, Pan Yaozhong and Cheng Xiao. 2010. Four prioritied reasearch areas of global change research that need to be strengthened in China // Gong P, ed. Review of Global Change Research, 1-11

Yang M M, Blake D R, Meinardi S, Vay S A, Choi Y, Rana M, Slate T, Sachse G W and Diskin G S. 2010. Chemical Composition of Tropospheric Air Mass Encountered During High Altitude Flight (> 11.5 km) over Antarctica at Latitude 86S During the 2009 Fall Operation Ice Bridge Field Campaign // American Geophysical Union, Fall Meeting 2010, abstract #A13B-0194, 0194